Hydrothermal Alteration Associated with Beryllium Deposits at Spor Mountain, Utah

Hydrothermal Alteration Associated with Beryllium Deposits at Spor Mountain, Utah

By DAVID A. LINDSEY, HAROLD GANOW, and WAYNE MOUNTJOY

BERYLLIUM-BEARING TUFFS IN WESTERN UTAH

*A description of the mineral and chemical
composition of beryllium-bearing tuff
at Spor Mountain, western Utah*

CONTENTS

ILLUSTRATIONS

TABLES

HYDROTHERMAL ALTERATION ASSOCIATED WITH BERYLLIUM DEPOSITS AT SPOR MOUNTAIN, UTAH

By DAVID A. LINDSEY, HAROLD GANOW, and WAYNE MOUNTJOY

ABSTRACT

The beryllium deposits at Spor Mountain occur in waterlaid tuff that contains carbonate clasts. Vitric and zeolitic tuffs are present outside the mineralized area whereas argillic and feldspathic tuffs are present within the mineralized area. Early alteration of tuff was characterized by argillization and addition of Si, Al, Fe, H_2O, F, Be, Li and many trace elements; advanced alteration was marked by feldspathization, fluorite-silica replacement of carbonate clasts, continued addition of many trace elements, and loss of water. As shown by potassium-feldspar and fluorite abundance, the alteration intensity at the Roadside beryllium deposit decreases with depth but shows a minor increase near the base of the tuff. The beryllium ore body and associated fluorite are near the top of the tuff and are underlain by a thick zone containing lithium-bearing trioctahedral montmorillonoid clay and associated calcite. Beryllium (as bertrandite), lithium, uranium, and other elements are concentrated in fluorite-rich nodules, and magnesium, lithium, and zinc are concentrated in trioctahedral montmorillonoid clay nodules. Most of the nodules are believed to be altered domomite clasts. Manganese oxide minerals occur as nodule coatings and fissure fillings.

The elements concentrated at Spor Mountain are tentatively believed to have been derived from a buried granitic pluton by fluorine-rich hydrothermal solutions. These solutions ascended into the overlying tuff where they reacted with carbonate clasts, releasing carbonate ions whose hydrolysis turned the solutions alkaline. Decreasing temperature probably caused precipitation of silica minerals and fluorite, producing and accompanying decrease in fluorine concentration. Increasing pH triggered potassium fixation and resulted in widespread feldspathization of the tuffs. Increasing pH, decreasing temperature, and decreasing fluorine concentration were variously responsible for the breakdown of stable metal fluoride complex ions and for the precipitation of minerals of beryllium, uranium, and other elements.

INTRODUCTION

Large beryllium deposits in western Utah are a significant part of the world's known beryllium resources (Griffitts, 1964). These deposits occupy a belt that extends west from the Sheeprock Mountains of Utah into Nevada (fig. 1) (Cohenour, 1963a). The deposits in Utah consist of beryl in granite of the Sheeprock Mountains (Cohenour, 1963b), bertrandite in tuff at Spor Mountain (Staatz and Griffitts, 1961), beryllium in tuff at the Honeycomb Hills (Montoya and others, 1964), beryl in pegmatites at Granite Peak (Fowkes, 1964), bertrandite in veins at Rodenhouse Wash (Griffitts, 1965), and beryl in veins and pegmatites in many places in the southern Deep Creek Mountains (Griffitts, 1964). The Spor Mountain deposits, discovered in 1959, contain large reserves of ore averaging less than 1 percent BeO. These ores are economically competitive with imported beryl because they are accessible by open-pit mining and the beryllium can be extracted by acid leaching. Brush Wellman Inc., began production in 1971 at their mill east of Delta, Utah, and the Spor Mountain deposits can be expected to provide a major source for beryllium in the future.

The purpose of this report is twofold: (1) to describe the mineralogy and chemical composition of the host tuff of the beryllium deposits at Spor Mountain, and (2) to define the principal alteration processes responsible for deposition of beryllium in tuff. This report, first in a series of reports on beryllium-bearing tuffs in western Utah, provides a basis for the recognition of alteration associated with beryllium deposits in tuff.

This report was written by the senior author, who is responsible for the observations and conclusions presented. Data on mineralogy and chemical composition used in preparing this report are available from the U.S. Department of Commerce National Technical Information Service, Springfield, Va. 22151 (Lindsey and others, 1973).

We thank the employees of Brush Wellman Inc., at Delta, Utah, for their cooperation and hospitality during fieldwork. W. R. Griffitts, U.S. Geological Survey, provided drill-hole samples obtained by him from the Vitro Minerals Corp. Kurt Buzard assisted the senior author in mineralogical studies and other laboratory work, and G. S. Bhatnagar, India Atomic Energy Commission, also participated in mineralogical studies for 2 weeks. Many other U.S. Geological Survey colleagues performed chemical analyses, and their help is acknowledged at appropriate places in the text.

GEOLOGIC SETTING

The Spor Mountain beryllium deposits are in the Basin and Range province in Juab County, Utah, on the east, south, and southwest sides of Spor Mountain (figs. 1 and 2).
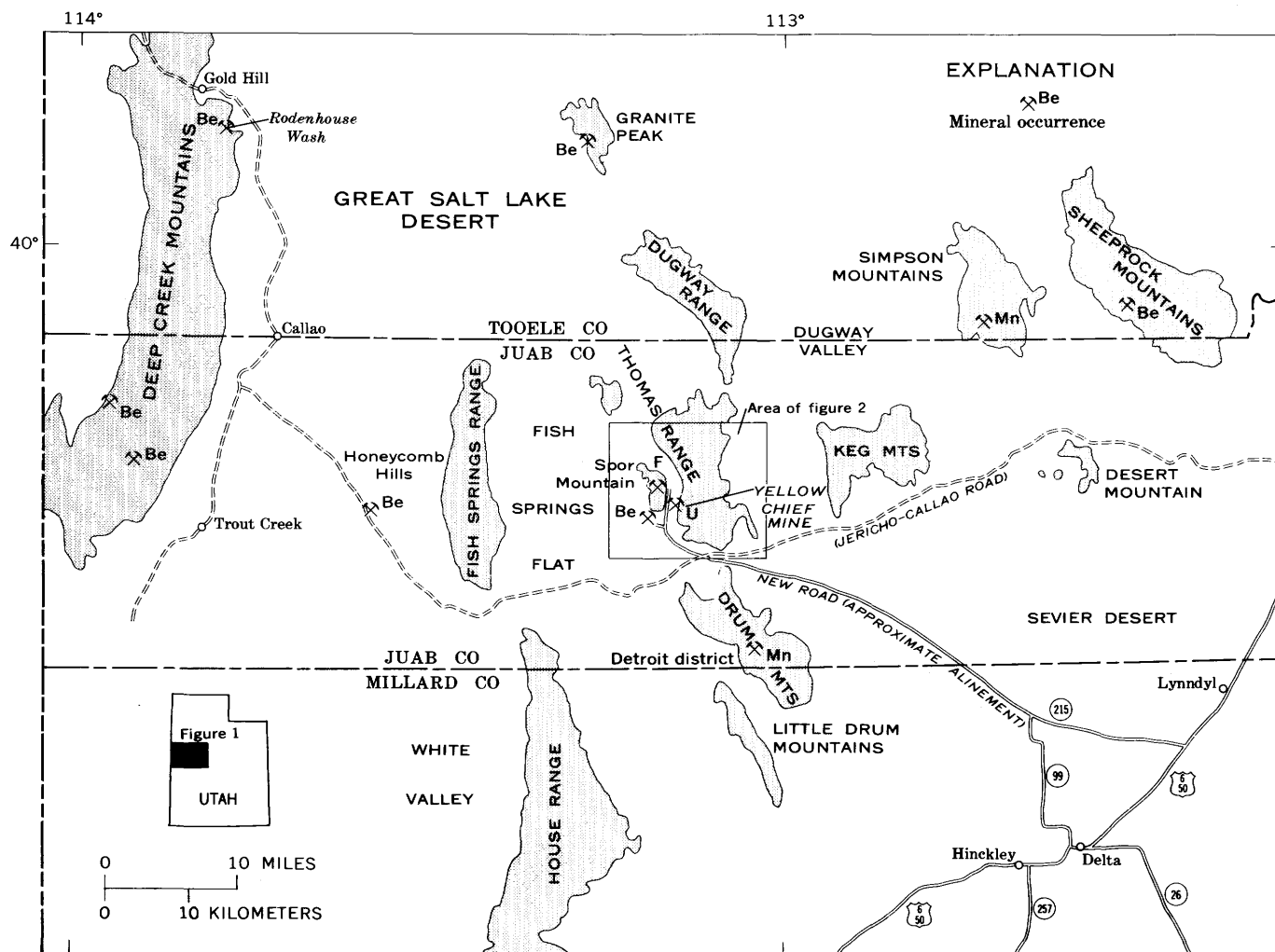
FIGURE 1. — Map showing location of Spor Mountain, other geographic features, and mineral occurrences mentioned in text.

Spor Mountain itself is an oval-shaped block of northwest-dipping Paleozoic rocks bounded on the east by a Basin-and-Range-type fault. East and northeast of Spor Mountain, and across a narrow valley termed "The Dell," is the Thomas Range. The Thomas Range, which includes Topaz Mountain and Antelope Ridge and adjoins the Dugway Range to the north and the Drum Mountains to the south, consists almost entirely of Tertiary volcanic rocks. Fish Springs Flat is west of the Thomas Range and Spor Mountain; the south end of Dugway Valley is to the east. Fish Springs Flat and Dugway Valley are underlain mainly by Lake Bonneville beds and alluvium.

The major rock units of concern in this report are, in ascending order, Paleozoic sedimentary rocks, the older volcanic rocks of Miocene(?) and older(?) age, and the younger volcanic rocks of Miocene(?) and Pliocene(?) age (fig. 2). The Paleozoic rocks, which crop out mainly on Spor Mountain and directly south of Topaz Mountain, are Early Ordovician to Late Devonian in age (Staatz and Carr, 1964, p. 31-53). The 3,950-foot-thick Paleozoic section at Spor

Mountain consists mostly of dolomite, but it also contains some quartzite, shale, and limestone (Staatz, 1963, p. M9). Numerous faults of diverse orientation cut the Paleozoic rocks on Spor Mountain. The older volcanic rocks crop out mainly in The Dell and in valleys in the eastern part of the Thomas Range. They correspond to Shawe's (1972) "middle assemblage of igneous rocks" and contain labradorite rhyodacite, rhyodacite, porphyritic rhyolite, quartz-sanidine crystal tuff, vitric tuff, and intrusive breccia (Staatz, 1963, p. M12-M18; Staatz and Carr, 1964, p. 75-86). Some of these rocks have been reinterpreted as ash-flow tuffs (Shawe, 1972). Minor amounts of tuffaceous sandstone and conglomerate are interbedded with the older volcanic rocks in The Dell. The younger volcanic rocks (younger assemblage of Shawe, 1972) consist of five sequences, each consisting, in ascending order, of vitric tuff (termed "water-laid" by Shawe, 1968, table 1), volcanic breccia, and topaz rhyolite (Staatz and Carr, 1964, p. 86-102). These sequences overlap one another, and the various sequences rest uncon-formably on the older volcanic rocks and on Paleozoic rocks

EXPLANATION

	ALLUVIUM	QUATERNARY
	YOUNGER VOLCANIC ROCKS	
	WATER-LAID TUFF BEDS. — Locally beryllium bearing	
	INTRUSIVE BRECCIA	TERTIARY
	OLDER VOLCANIC ROCKS	
	MARINE CARBONATE AND CLASTIC ROCKS	PALEOZOIC

—————— CONTACT

—————— FAULT. — Dotted where concealed

BERYLLIUM DEPOSIT. — Area underlain by beryllium-bearing tuff. Approximately located
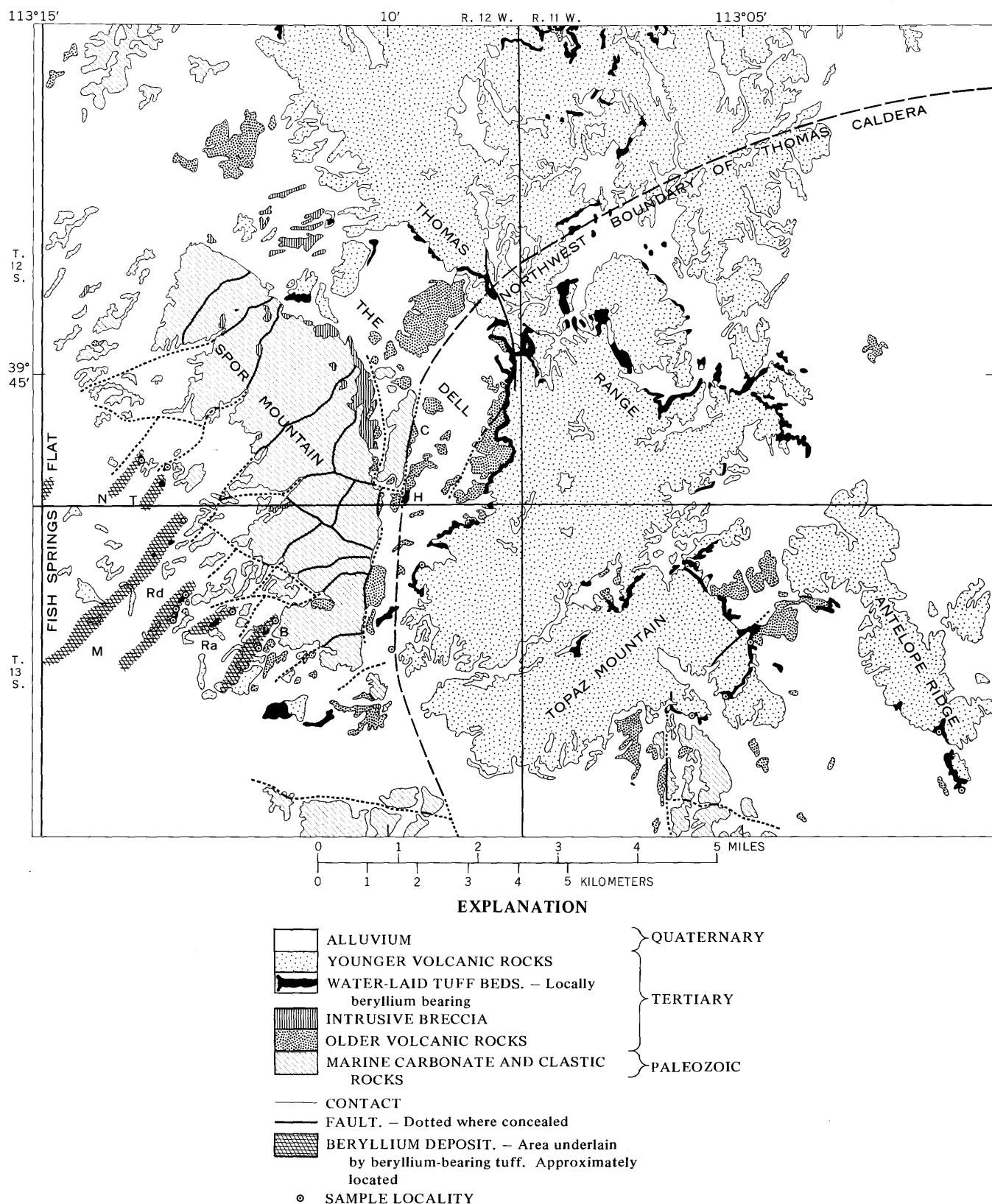
⊙ SAMPLE LOCALITY

FIGURE 2. — Geologic setting, beryllium deposits, and sample localities in Miocene(?) and Pliocene(?) water-laid tuff at Spor Mountain and the Thomas Range. Map slightly modified from Shawe (1968, fig. 1). Beryllium deposits shown on the map are North End (N), Tauras (T), Monitor (M), Roadside (Rd), Rainbow (Ra), Blue Chalk (B), Hogsback (H), and Claybank (C).

in some places. The younger volcanic rocks make up most of the Thomas Range and also crop out in parts of The Dell and southwest of Spor Mountain. The older volcanic rocks were deposited prior to formation of the Thomas caldera; the younger volcanic rocks postdate collapse of the caldera (Shawe, 1972).

The beryllium deposits occur mostly in the water-laid vitric tuffs of the younger group, although at least one deposit (Claybank) is known to occur in vitric tuff in the older group, and traces of mineralization are present in the Paleozoic dolomites (Staatz, 1963, p. M25). The vitric tuff of the younger group exceeds 300 feet in thickness in only a few places and may be entirely missing at some locations (Williams, 1963, p. 48; Staatz and Carr, 1964, p. 86-87). The tuff is termed "water-laid" because stratification and sorting of clasts characterize most outcrops. The tuff consists mostly of volcanic detritus or its alteration products, but at the base of Topaz Mountain it contains some limestone clasts, and southwest of Spor Mountain, abundant dolomite clasts that are commonly altered to calcite, silica minerals, fluorite, and clay. In the area of beryllium mineralization southwest of Spor Mountain, Williams (1963, p. 50-51) divided the tuff into three members. (1) The lower member comprises about two-thirds of the total thickness and is characterized by abundant dolomite clasts, (2) the middle member is present locally and is marked by welding, and (3) the upper member comprises one-third of the total thickness and is marked by much-altered carbonate clasts and by volcanic rock fragments that are more abundant than in the lower member. As will be shown later, the upper and lower members in part are characterized by differing degrees of alteration.

Mineralization also may have been controlled by faults which cut the younger volcanic rocks in a few places, notably southwest of Spor Mountain and along the east side of The Dell. Southwest of Spor Mountain, southwest-trending faults can be projected from the Paleozoic rocks into the younger volcanic rocks (fig. 2), where they are believed to have controlled the orientation of tuff-filled paleovalleys and to have served also as conduits for mineralizing fluids (Williams, 1963, p. 47; Griffitts, 1964, p. 73-74; Shawe, 1968, p. 1160). East of Spor Mountain, the Claybank and Hogsback prospects reveal zones of beryllium mineralization along a prominent north-trending fault (Staatz, 1963, p. M27).

The beryllium deposits are closely related spatially, and probably genetically, to fluorite, uranium, and manganese deposits (fig. 1). All these deposits occur around the periphery of the Thomas caldera (Shawe, 1972, fig. 2). Fluorite in commercial quantities occurs in pipes and in a few veins on Spor Mountain (Thurston and others, 1954, p. 24-45); uranium is present in some of the pipes (Staatz and Carr, 1964, p. 135-139). A uranium deposit of commercial significance (Yellow Chief) occurs in tuffaceous sandstone and conglomerate in The Dell (Staatz and Carr, 1964, p.

148-157). Sizable manganese deposits are present in the Drum Mountains to the south (Crittenden and others, 1961).

PREVIOUS MINERALOGICAL AND GEOCHEMICAL WORK

Most of the previous mineralogical and geochemical work has been limited in extent and has been directed toward identifying the various mineral phases in the tuff and beryllium ore. Staatz and Griffitts (1961), Staatz (1963), and Shawe (1968) described the mineralogy of both fresh and altered tuff; they noted that the altered tuff consists mainly of clay, silica minerals, fluorite, and feldspar. The occurrence of much of the beryllium as bertrandite $(Be_4Si_2O_7(OH)_2)$ or some closely related mineral was recognized by Staatz and Griffitts (1961, p. 947). They and Montoya, Havens, and Bridges (1962) found that bertrandite is concentrated in fluorite-silica nodules as well as being dispersed in the tuff. The only quantitative mineralogical work is that of Montoya, Havens, and Bridges (1962), who reported abundant well-crystallized cristobalite, feldspar, and saponite in the altered tuff, and who independently discovered the presence of bertrandite.

Early chemical studies showed the association of F, U, and Mn with beryllium (Staatz and Griffitts, 1961). Fluorine was shown to accompany beryllium closely in three drill holes through the beryllium ore body (Griffitts and Rader, 1963). Unusually large amounts of lithium were found to be more widespread than beryllium in the altered tuff (Shawe and others, 1964; Shawe, 1968, p. 1156). At the Roadside deposit, Shawe (1968) found that MgO, F, B, Cr, and Tl are more abundant in beryllium-rich tuff than in beryllium-poor tuff. In samples from a section in the Rainbow deposit and in samples obtained from four widely scattered drill holes southwest of Spor Mountain, beryllium was found to be abundant in the upper part of the tuff and was accompanied by anomalous Pb, Zn, Cd, Mn, As, F, and U (Park, 1968, p. 30-41).

ALTERATION OF THE WATER-LAID TUFF

To acquire some idea of the total range of mineral and chemical composition of the tuff, we selected 14 samples from seven unmineralized localities in the Thomas Range (at Antelope Ridge, Topaz Mountain, and The Dell) and 16 samples from eight mineralized localities representing the following beryllium prospects southwest of Spor Mountain: The Blue Chalk, an unnamed prospect south of the Blue Chalk, the Rainbow, the Roadside (three localities), the Taurus, and the North End. Samples from the Monitor prospect were also studied petrographically, but were not analyzed. Two samples were collected from each locality, one each from the lower and upper parts of the tuff bed or from opposite ends of the prospect. No attempt was made to sample beryllium deposits of ore grade at this stage in the study. A part of each sample was reserved for a reference hand specimen and thin section; the 30 samples were then

placed in random order prior to mineralogical and chemical analysis.

All 30 samples are from the younger volcanic group, but the unmineralized tuffs were selected from three different tuff units. The mineralized tuff southwest of Spor Mountain represents a fourth tuff unit and differs from the unmineralized tuff in that it contains dolomite clasts and their alteration products calcite and fluorite. Nevertheless, the matrix of the mineralized tuff probably was very similar to that of the unmineralized tuff, and the latter is the best available rock from which to infer the original mineralogy and trace-element content of the water-laid tuffs.

PETROGRAPHY OF UNMINERALIZED TUFF

Fourteen samples from three different unmineralized tuff units were studied in hand specimen, in thin section, and by whole-rock X-ray diffraction. Most of the tuff contains 1-14 percent pyrogenic crystals, as much as 80 percent pumice fragments, 2-26 percent volcanic rock fragments, sparse chert, quartzite, and sandstone, and, locally, a small percentage of obsidian and limestone fragments in a vitric or zeolitic matrix. Pyrogenic crystals consist of 1-14 percent quartz, 0-5 percent sanidine, 0-2 percent plagioclase, 0-1 percent biotite, and trace amounts of magnetite, ilmenite, topaz, sphene, and zircon. Quartz and sanidine occur

mainly as euhedral grains, many of which have ·resorbed outlines and are broken. X-ray diffraction (method of Wright, 1968, fig. 3) indicates that the sanidine is cryptoperthitic and has a structure near that of low sanidine. Measurement of 2V suggests an overall composition near Or_{70}. Measurement of albite twin extinction angles by the Michél-Levy method indicates that some plagioclase is oligoclase, but that a more calcic zoned plagioclase is also present. Biotite and plagioclase are commonly euhedral, but broken plagioclase crystals are common. Biotite is brown, pleochroic, and typically fresh. Volcanic rock fragments contain varying amounts of quartz, sanidine, zoned plagioclase (some of which is andesine), and lesser amounts of biotite, amphibole, and opaque minerals scattered about in a fine-grained, locally spherulitic matrix which, as shown by X-ray diffraction, consists of potassium feldspar and α-cristobalite.

The unmineralized samples that were examined are vitric and zeolitic tuffs (fig. 3A and B; table 1). Fresh vitric tuffs are present at the south end of The Dell, where they are composed mainly of glassy, vesicular pumice fragments as large as several inches across. Lesser quantities of volcanic rock fragments and obsidian, a few crystals, and a matrix of undeformed glass shards accompany the pumice. Volcanic rock fragments have a devitrified matrix, whereas accom-

TABLE 1. — Comparison of the density, porosity, mineral composition, and chemical composition of unmineralized and mineralized water-laid tuff, Spor Mountain and the Thomas Range, Utah

[All values are medians (50th percentiles); where the median falls below the limit of detection, or where large variation is present, the maximum value (in parentheses) is recorded also. Mineralogy is by X-ray diffraction. Analytical methods and analysts are as follows: SiO_2 and Al_2O_3 determined by fusion X-ray fluorescence by J. S. Wahlberg and M. W. Solt; $FetO_3$, MgO, CaO, Li, and Rb determined by atomic absorption by Johnnie Gardner and Violet Merritt; Cs determined by atomic absorption by Wayne Mountjoy; In and Tl determined by atomic absorption by A. L. Hubert; Na_2O and K_2O determined by flame photometer by Johnnie Gardner and Violet Merritt; LOI determined by drying at 900°C for 1 hour by R. L. Rahill; CO_2 determined gasometrically by I. C. Frost; Cl determined nephelometrically with mercuric nitrate by H. H. Lipp; F determined volumetrically by Johnnie Gardner; and eU determined by Beta scaler by E. J. Fennelly. All elements from B through Zr determined by direct reader spectrograph by R. G. Havens. Elements looked for but not found, and their detection limits, in parts per million, are Ag, 4; Au, 20; Bi, 20; Cd, 100; Co, 8; Ge, 100; Mo, 20; Pd, 10; Re, 70; Sb 300; and W, 500]

	Unmineralized tuff		Mineralized tuff			Unmineralized tuff		Mineralized tuff	
	Vitric	Zeolitic	Argillic	Feldspathic		Vitric	Zeolitic	Argillic	Feldspathic
Number of samples _ _ _ _ _	10	4	8	8	Number of samples _ _ _ _ _	10	4	8	8
Density (grams per cubic centimeter) and porosity (percent)					**Chemical composition (weight percent) — Continued**				
Powder density _ _	2.41	2.43	2.47	2.52	H_2O^a _ _ _ _ _ _ _ _	4.60	7.51	7.36 (1.15)	5.53
Bulk density _ _ _ _	1.47	1.73	1.85	1.82	Cl _ _ _ _ _ _ _ _ _ _	.22 (0.94)	.07 (0.57)	.45 (1.15)	.31 (1.75)
Porosity _ _ _ _ _ _	39.0	28.8	24.7	27.8	F _ _ _ _ _ _ _ _ _	.17	.11	1.22	1.82
Mineral composition (weight percent)					**Chemical composition (parts per million)**				
Montmorillonoid[1] _	_ _ _ _ _ _ _	<1 (5)	66	9	Cs _ _ _ _ _ _ _ _ _	20	10	89	38
Mica[2] _ _ _ _ _ _ _	_ _ _ _ _ _ _	2	1	<1	In _ _ _ _ _ _ _ _ _	<.2	<.2	<.2 (1.5)	<.2 (18.4)
Clinoptilolite _ _ _	14	65	<1 (40)	_ _ _ _ _ _ _	Li _ _ _ _ _ _ _ _ _	75	55	230	315
Quartz _ _ _ _ _ _ _	4	95	5	9	Rb _ _ _ _ _ _ _ _ _	305	295	395	620
α-cristobalite[3] _ _	3	4	5	25	Tl _ _ _ _ _ _ _ _ _	2.5	2.4	3.5 (19.9)	6.1 (54.0)
Potassium feldspar[4] _ _ _ _ _	11	18	18	52	eU _ _ _ _ _ _ _ _ _	45	45	65	85
Calcite _ _ _ _ _ _	1 (12)	<1	1 (23)	_ _ _ _ _ _ _	B _ _ _ _ _ _ _ _ _ _	34	<30 (39)	60	60
Dolomite _ _ _ _ _	_ _ _ _ _ _ _	_ _ _ _ _ _	1 (5)	_ _ _ _ _ _ _	Ba _ _ _ _ _ _ _ _ _	160	205	120	70
Fluorite _ _ _ _ _ _	<1	1	3	4	Be _ _ _ _ _ _ _ _ _	7	7	105	14 (250)
Halite _ _ _ _ _ _ _	<1	_ _ _ _ _ _	<1	1	Cr _ _ _ _ _ _ _ _ _	9	8	5	<5
Glass[5] _ _ _ _ _ _ _	66	<1	<1	_ _ _ _ _ _ _	Cu _ _ _ _ _ _ _ _ _	3	3	3	3 (43)
					Fe _ _ _ _ _ _ _ _ _	8,700	7,350	9,100	10,500
					Ga _ _ _ _ _ _ _ _ _	28	27	44	50
					La _ _ _ _ _ _ _ _ _	53	25	70	76
Chemical composition (weight percent)					Mn _ _ _ _ _ _ _ _ _	700	310	510 (3,400)	805 (8,000)
					Nb _ _ _ _ _ _ _ _ _	30	25	66	71
SiO_2 _ _ _ _ _ _ _ _	69	68	64	64	Ni _ _ _ _ _ _ _ _ _	<7 (7)	<7	<7 (7)	<7
Al_2O_3 _ _ _ _ _ _ _	10	10	11	11	Pb _ _ _ _ _ _ _ _ _	34	30	37	42
$FetO_3$ _ _ _ _ _ _ _	1.06	1.06	1.28	1.30	Sc _ _ _ _ _ _ _ _ _	<10	<10	<10 (14)	<10 (30)
MgO _ _ _ _ _ _ _	.74	.52	1.98	1.42	Sn _ _ _ _ _ _ _ _ _	<20 (20)	<20	34	52
CaO _ _ _ _ _ _ _	1.83 (9.00)	2.05	2.46 (14.00)	2.90	Sr _ _ _ _ _ _ _ _ _	195	230	210	145
Na_2O _ _ _ _ _ _ _	2.78	1.99	2.40	2.39	Ti _ _ _ _ _ _ _ _ _	585	565	350	315
K_2O _ _ _ _ _ _ _	4.22	4.34	2.69	5.10	V _ _ _ _ _ _ _ _ _	14	13	17	11
LOI[6] _ _ _ _ _ _ _	5.8	8.1	8.6	5.5	Y _ _ _ _ _ _ _ _ _	29	30	75	120
CO_2 _ _ _ _ _ _ _	.50 (6.11)	.30	.45 (9.91)	.06	Zn _ _ _ _ _ _ _ _ _	<300	<300	<300 (340)	150 (1,600)
					Zr _ _ _ _ _ _ _ _ _	67	69	73	78

[1] Dioctahedral montmorillonoid clay; quantity determined by difference.
[2] Pyrogenic biotite plus secondary sericite.
[3] Includes some opal.
[4] Pyrogenic sanidine plus secondary potassium feldspar.

[a] Quantity determined by difference.
[b] Total Fe as Fe_2O_3.
[6] Loss on ignition (LOI) at 900°C for 1 hour.
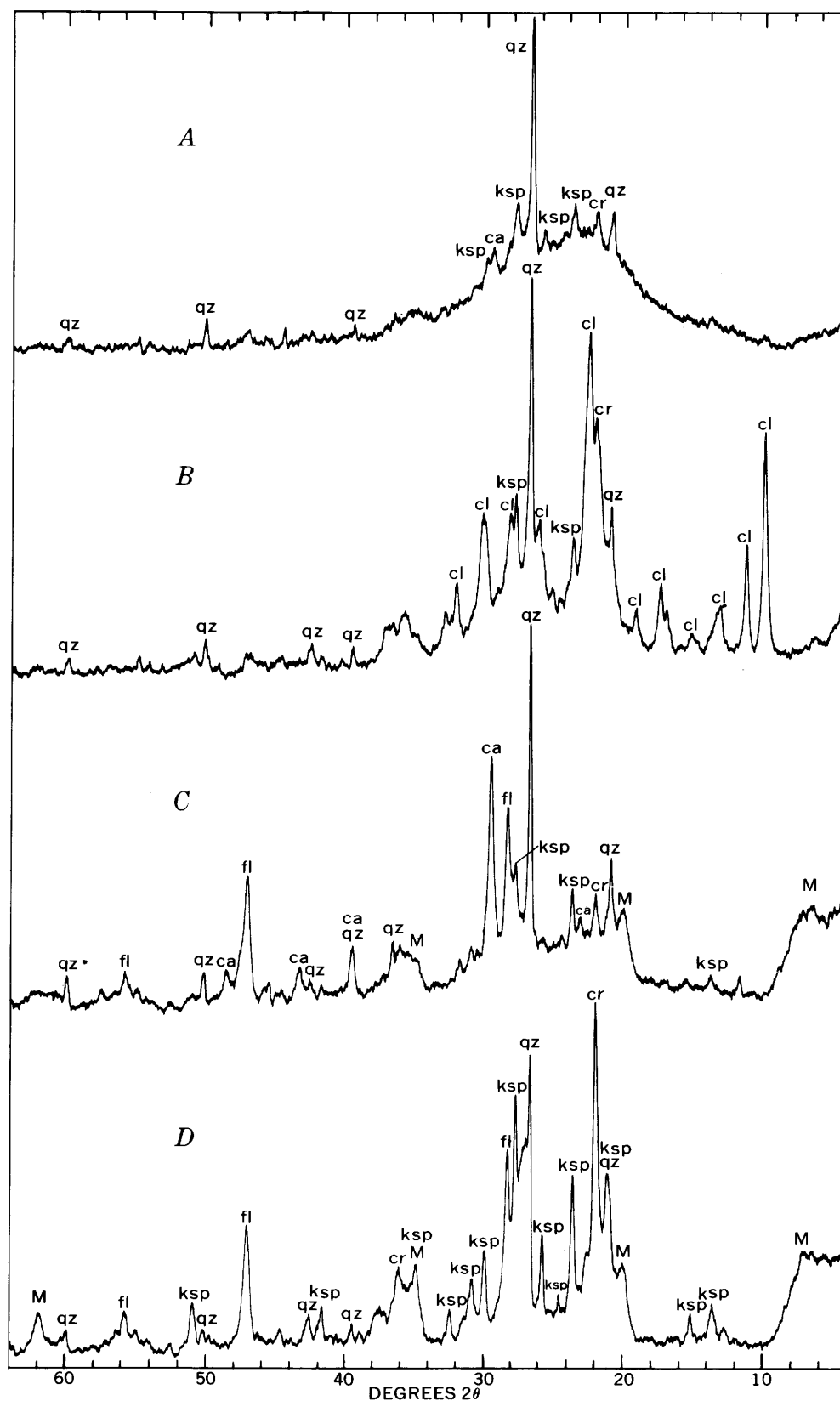[c] LOI minus CO_2.

FIGURE 3. — Whole-rock X-ray diffractograms of water-laid tuff at Spor Mountain and the Thomas Range:
A, Vitric tuff. *B*, Zeolitic tuff. *C*, Argillic tuff. *D*, Feldspathic tuff. Abbreviations: ca, calcite; Cl, clinop-
tilolite; cr, cristobalite; fl, fluorite; ksp, potassium feldspar; M, montmorillonoid; qz, quartz.

panying obsidian, pumice, and shards are composed of fresh glass. Some vitric tuff samples also contain fine-grained calcite in the matrix and sparse microcrystalline to coarsely crystalline limestone fragments. The matrix calcite is concentrated generally in zones around pumice fragments.

Zeolitic tuff is recognizable by whole-rock X-ray diffraction (fig. 3B) and is characterized in thin section by the almost complete destruction of glass and vesicular pumice. Relict pumice vesicles are common, however, and are outlined by clear to light-brown, birefringent montmorillonoid clay flakes. Fuzzy brown material of very fine grain size is also common and is probably clay. Much of the matrix is composed of very small low-birefringence grains shown by X-ray diffraction to be almost entirely clinoptilolite. Identification as clinoptilolite was confirmed by heating samples (method of Mumpton, 1960); no destruction or change in structure was observed. Some zeolitic tuff contains abundant calcite, both as limestone pebbles and smaller clasts and as redistributed coarsely crystalline cement. Calcite is particularly abundant on the east side of Topaz Mountain, where some limestone pebbles were seen in outcrops.

PETROGRAPHY OF MINERALIZED TUFF

Sixteen samples from the mineralized tuff southwest of Spor Mountain were studied in hand specimen, thin section, and by whole-rock X-ray diffraction; these observations were supplemented by examination of some additional samples. The mineralized tuff contains about 8-21 percent pyrogenic crystals accompanied by variable amounts of pumice, volcanic rock, and altered dolomite pebbles in a matrix which varies from brown to pink to cream. The pyrogenic crystals include 1-5 percent quartz, 2-11 percent sanidine, 0-2 percent plagioclase, and 0-1 percent biotite. Many grains are quite fresh and unaltered, with crystal form and composition similar to those of unmineralized tuff. Biotite in the mineralized tuff, in contrast to that in unmineralized tuff, is commonly black and appears oxidized. Pumice, volcanic rock, and dolomite fragments exhibit a wide variation in degree of alteration. Clay which swells upon weathering to produce popcornlike texture similar to bentonite is ubiquitous, and veinlets and void fillings of calcite, opal, and manganese oxides are common locally.

Argillic and feldspathic alteration characterize the mineralized tuffs (fig. 3C and D; table 1). Much of the argillic alteration was incomplete, with vitric and zeolitic components commonly abundant. The feldspathic alteration is regarded as a more advanced stage, inasmuch as it was generally accompanied by complete destruction of unstable prealteration components. It must be stressed that these facies represent end members; all the samples studied were designated argillic or feldspathic tuff, but some clearly show attributes of both. Assessment of the degree of alteration is best made by whole-rock X-ray diffraction, but examination of thin sections is often necessary to detect unaltered glass.

Argillic tuff can be readily identified by X-ray diffraction (fig. 3C). It is characterized by as much as 80 percent montmorillonoid clay and 1-5 percent fluorite, by the presence of dolomite, calcite, and clinoptilolite in some samples, and by not more feldspar than the 20 percent or less which was probably present prior to mineralization (comparable to unmineralized tuff potassium feldspar content). The clay is a dioctahedral montmorillonoid similar to montmorillonite (Ross and Hendricks, 1945, table 1); it swells when saturated with glycerol, collapses upon heating to 300°C, and has an 060 d-spacing of 1.495 A. A trioctahedral montmorillonoid clay (060 = 1.515 A), which has a chemical composition similar to that of hectorite (Ames and others, 1958) but which also contains as much as 1 percent zinc, is also present locally but was not identified in the samples under discussion. Argillic tuff, as seen under the microscope, retains many fragments of fresh glassy pumice, volcanic rock, and carbonate rock. The glass is generally too sparse to be detected by X-ray diffraction. Clay, sericite, opal, and fine-grained (0.01-0.05 mm) anhedral fluorite are common and have replaced both matrix and pumice fragments. Euhedral halite was identified in a few samples and probably accounts for anomalous chlorine detected in some samples. Hand specimens show a wide range of dolomite clast alteration, from snow-white bleached calcite to complete replacement by quartz, opal, purple fluorite, and clay (fig. 4A, and B). Clay commonly rims the calcite fragments, but in the same sample other pebbles may be completely replaced by opal, fluorite, and clay. The bleached calcite is mainly microcrystalline, and locally it contains reflect invertebrate fossil fragments. Layered void fillings of clay, calcite spar, and opal (passing toward void center), more complex fillings of the same minerals, and calcite veinlets indicate that redistribution of calcite was widespread (fig. 4C). Other features are concentrations of fine-grained sparry calcite and sericite around rock fragments (fig. 4D), voids filled with euhedral fluorite and anhedral microcrystalline quartz (fig. 4E), clay and fibrous chalcedony(?) filling pumice vesicles, and fluorite filling fresh glassy pumice vesicles (fig. 4F). Manganese oxides, in crosscutting veinlets, appear to be among the last minerals formed.

Feldspathic tuff can also be readily identified by X-ray diffraction by the appearance of abundant potassium feldspar (≥20 percent) and, in some samples, 10-30 percent α-cristobalite (fig. 3D). Cristobalite is arbitrarily distinguished from opal in this report by the sharp X-ray diffraction peaks as shown in figure 3D; the peaks are very broad for opal, although gradations between sharp and broad are common. Similar gradational series have been produced by heating opal (Eitel, 1957, fig. 15; Franks and Swineford, 1959, p. 190-193). Montmorillonoid clay (as much as 40 percent) and fluorite (1-8 percent) are abundant whereas glass, clinoptilolite, and calcite usually are not,
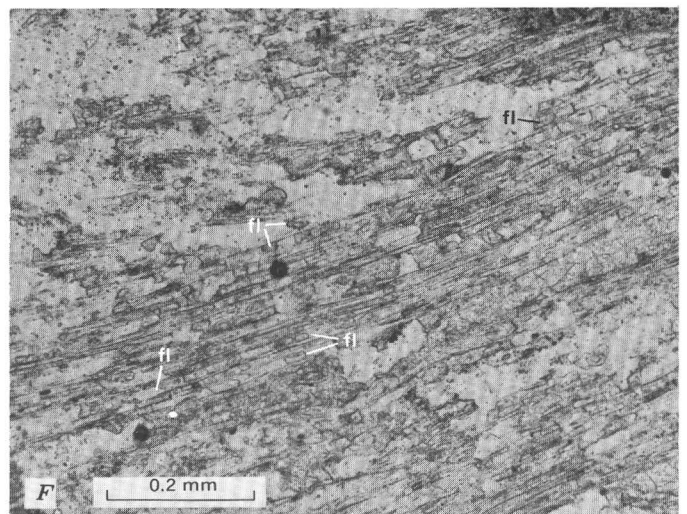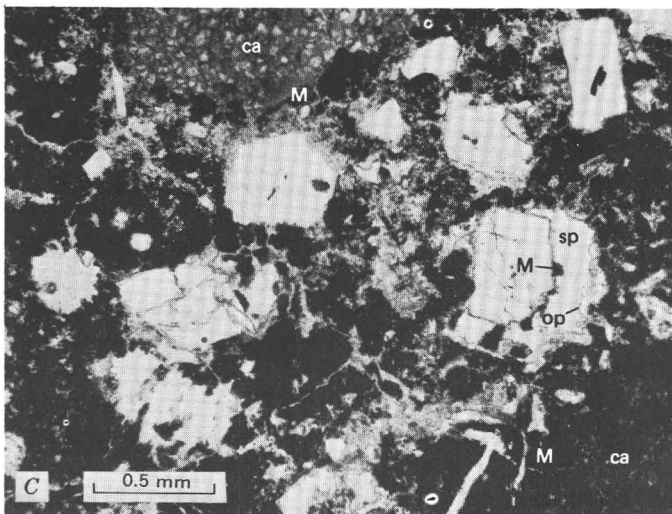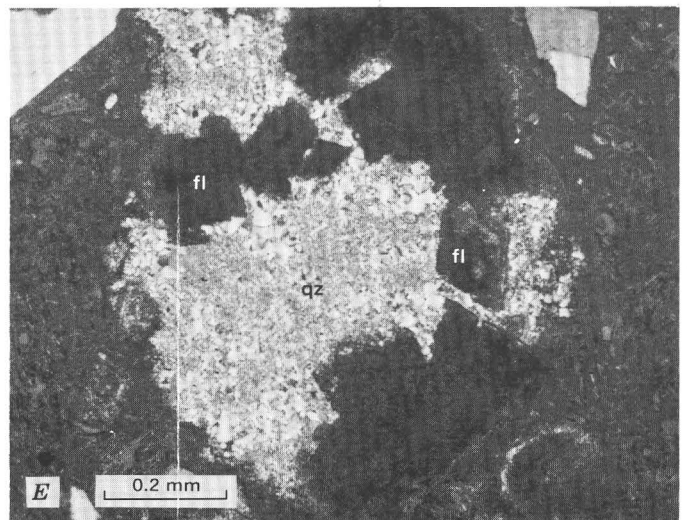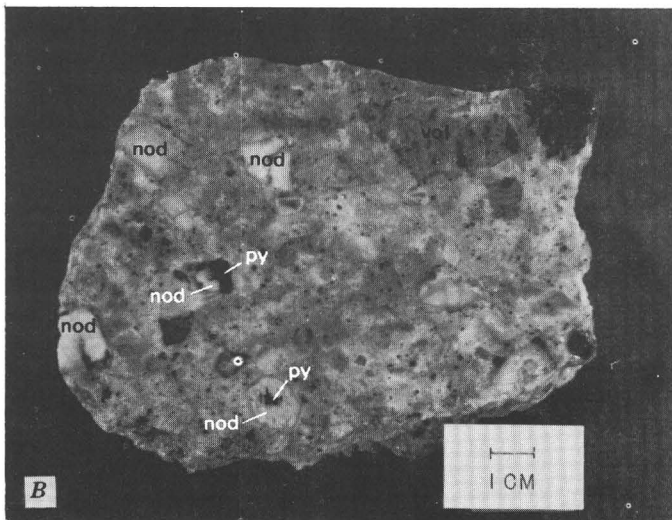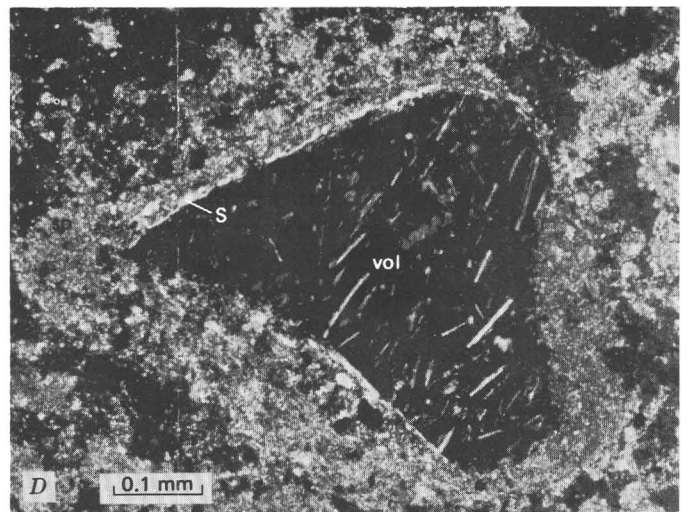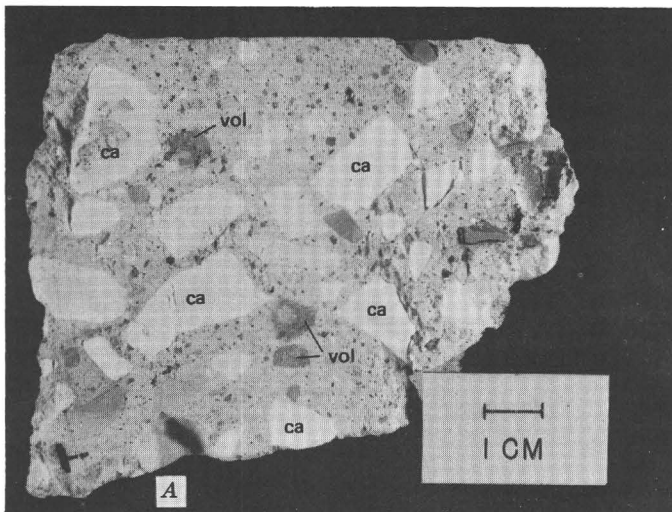
though remnant calcite may persist in altered clasts. Hand specimens appear to be intensely altered because former dolomite pebbles are replaced by quartz, opal, and purple fluorite or by clay, fluorite, and manganese oxides (fig. 5*A*, and *B*), but X-ray study is necessary to verify feldspathic alteration. Ragged matrix-carrying feldspar overgrowths on sanidine are commonplace (fig. 5*C* and *D*), and clay, potassium feldspar, cristobalite, sericite(?), and fine-grained anhedral fluorite replace both relict pumice and matrix. In some samples, the potassium feldspar and cristobalite occur as spherulites and fibrous masses that have replaced pumice and matrix alike. These closely resemble the devitrified textures of potassium feldspar and cristobalite noted in volcanic rock fragments of unmineralized tuff and welded tuffs from other areas (Ross and Smith, 1961, p. 26-38). Relict pumice texture is still visible in some samples of the feldspathic tuff, and concentric rims of fibrous chalcedony(?) and clay enclose pumice vesicle fillings of microcrystalline quartz and sericite (fig. 5*E*). Sericite (identified by X-ray as well as optically) rims volcanic rock fragments (fig. 5*F*) and opaque grains, and a similar micaceous mineral, probably also sericite, rims fine-grained fluorite in the matrix. Everywhere, manganese oxides in veinlets crosscutting matrix appear to be among the last minerals formed.

CHEMICAL COMPOSITION

Caution must be used in comparing the composition of mineralized tuff with that of unmineralized tuff, as shown in table 1, because only the mineralized tuff originally contained abundant dolomite clasts. Consequently, the proportion of major components, especially SiO_2, is somewhat diluted by the presence of locally abundant CaO, MgO, CO_2, and F, all due to dolomite or its alteration products calcite and fluorite. The most striking chemical differences appear in the trace-element content, however, and these are not due to dilution because the mineralized tuffs are considerably enriched in many trace elements. The elements Cs, Li, Rb, Tl, eU, B, Be, Ga, La, Mn, Nb, Sc, Sn, Y, and Zn show a concentration of about twofold or more in mineralized tuff over unmineralized tuff; Ba, Cr, and Ti are less abundant.

Argillic and feldspathic tuffs differ in important respects and reflect the mineralogical differences which formed the basis of their classification. As alteration progressed from the argillic to the feldspathic stage, CO_2 was removed and F added as dolomite and calcite were converted to fluorite, and K_2O shows a large increase from less than 3 to more than 5 percent as glass, zeolite, and clay were converted to potassium feldspar. Also noteworthy is the decrease in H_2O content of feldspathic tuff.

Further comparison of the chemistry of the argillic and feldspathic tuffs shows that additional concentration of many trace elements occurred as alteration proceeded toward complete feldspathization. Li, Rb, Tl, eU, Mn, Sn, Y, Zn, and perhaps Ga, La, and Nb continued to be concentrated, although the differences are not as marked as those between unmineralized and mineralized tuff. The trace elements Cs, Ba, Sr, and perhaps Be, Cr, and Ti declined in abundance as alteration proceeded. Beryllium abundance appears to be extremely variable; analyses of individual samples show that it may be concentrated in either the argillic or the feldspathic stages of alteration.

ALTERATION PATTERNS AT THE ROADSIDE ORE DEPOSIT

In order to examine possible alteration patterns in mineralized tuff, drill cuttings from holes 1 and 2 at the Roadside deposit (Griffitts and Rader, 1963, fig. 1) were studied by X-ray diffraction. No thin-section observations were possible owing to the finely ground condition of the cuttings. Griffitts and Rader showed the extent of beryllium ore cut by the drill holes and demonstrated the close association of beryllium with fluorine in the upper part of the tuff. Alteration patterns, details of the X-ray mineralogy, and the beryllium-abundance data of Griffitts and Rader are presented in figure 6.

Both mineralogy and beryllium content are to a large extent stratigraphically controlled (fig. 6*A* and *B*). Primary stratigraphic features are evident in the ratio of volcanic to dolomite detritus present (fig. 6*C*, and *D*). Both holes reveal that the original tuff contained an upper, dolomite-poor interval of about 50 feet in thickness and a lower, dolomite-rich interval comprising the remainder. Within the dolomite-rich interval, several horizons of maximum dolomite clast content are clearly discernible and correlative between holes.

The ensuing alteration of the tuff was also concordant to the stratigraphy. Intensity of alteration of the dolomite clasts progresses upward in the tuff, passing from unaltered dolomite to calcite to fluorite. Small amounts of fluorite also occur near the bottom of the tuff. Alteration of the volcanic fraction was most intense in the upper 60 feet and the lower 30 feet of the tuff, where potassium feldspar is most abundant. Abundant lithium-bearing trioctahedral montmorillonoid clay (060=1.515 A) coincides with abundant calcite over an interval exceeding 60 feet in thickness

FIGURE 4. — Features of argillic alteration in water-laid tuff at Spor Mountain. *A*, Specimen showing angular fragments bleached to white calcite (ca) and scattered pumice and volcanic rock fragments (vol, Matrix is mainly glass and montmorillonoid clay. *B*, Specimen showing nodules (nod) with opal-fluorite rind and dioctahedral montmorillonoid clay interiors crosscut by pyrolusite (py). Unaltered volcanic cobble (vol) also present. Matrix is mainly clinoptilolite. *C*, Photomicrograph showing montmorillonoid clay rinds (M) on bleached calcite clasts (ca) accompanied by void fillings of opal (op), montmorillonoid clay (M), and sparry calcite (sp). *D*, Photomicrograph showing volcanic rock fragment (vol) rimmed by sericite (s) and fine-grained sparry calcite (sp). *E*, Void fillings of euhedral fluorite (fl) and anhedral microcrystalline quartz (qz). *F*, Fine-grained fluorite (fl) filling glassy pumice vesicles. *A* and *C* are from Monitor pit; *B* is from Roadside pit; *D*, *E*, and *F* are from small pit south of Blue Chalk prospect. *C*, *D*, and *E* under crossed polars; *F* under plain light.
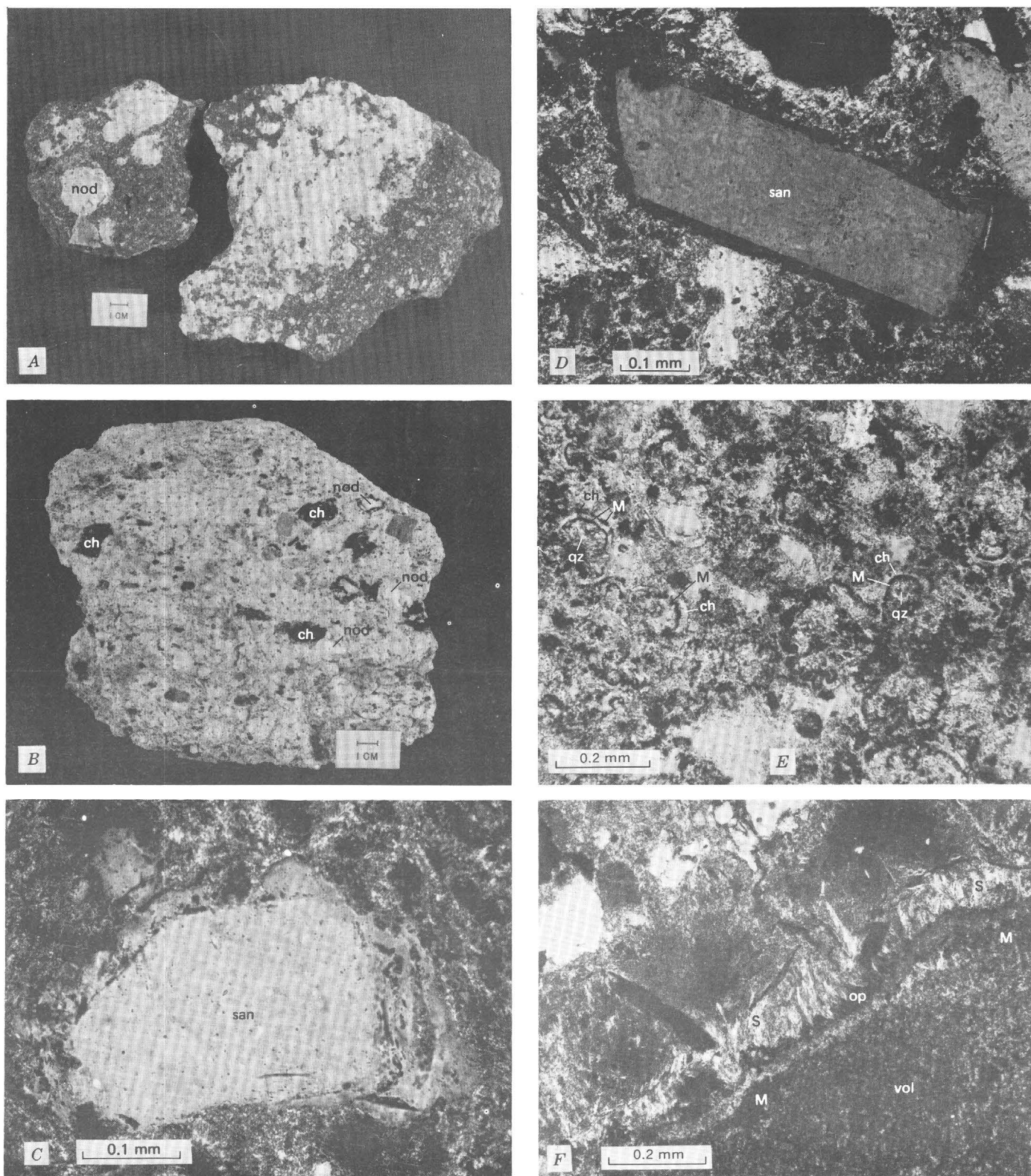
FIGURE 5. — Features of feldspathic alteration in water-laid tuff at Spor Mountain. A, Specimen with light-pink nodules (nod) composed of dioctahedral montmorillonoid clay, opal, and fluorite in dark matrix of clay, cristobalite, quartz, and potassium feldspar. Light nodules on left contain as much as 3,000 ppm (parts per million) Be. B, Specimen with light-colored nodules (nod) composed of dioctahedral montmorillonoid clay, opal, and fluorite in light-colored matrix of same minerals plus quartz, abundant potassium feldspar, and mica. Dark nodules are chalcophanite (ch). Both light and dark nodules contain as much as 5,000 ppm Be. C and D, Photomicrographs of pyrogenic sanidine crystals (san) with potassium feldspar overgrowths enclosing remnants of tuff matrix. E, Photomicrograph of relict pumice vesicles with concentric rims of fibrous chalcedony(?) (ch) and clay (M) and fillings of microcrystalline quartz (qz) and sericite. F, Photomicrograph of volcanic rock fragment (vol) rimmed by clay (M) and sericite (S). Dark band in middle of sericite is unidentified opaque mineral (op). A — D and F are from the Roadside pit; E is from the Blue Chalk prospect. All photomicrographs under crossed or partly crossed polars.

indicating that the clay formed in response to dedolomitization of the clasts. Quartz shows no concentration or trend, but cristobalite is clearly most abundant in the lower half and in the extreme upper 20 feet of the tuff, where it roughly parallels but does not coincide exactly with the distribution

of secondary potassium feldspar. Remnant clinoptilolite is present locally.

Beryllium is most closely associated with the distribution of fluorite (fig. 6A and B), as demonstrated by Griffitts and Rader (1963). Beryllium is mainly concentrated in the upper
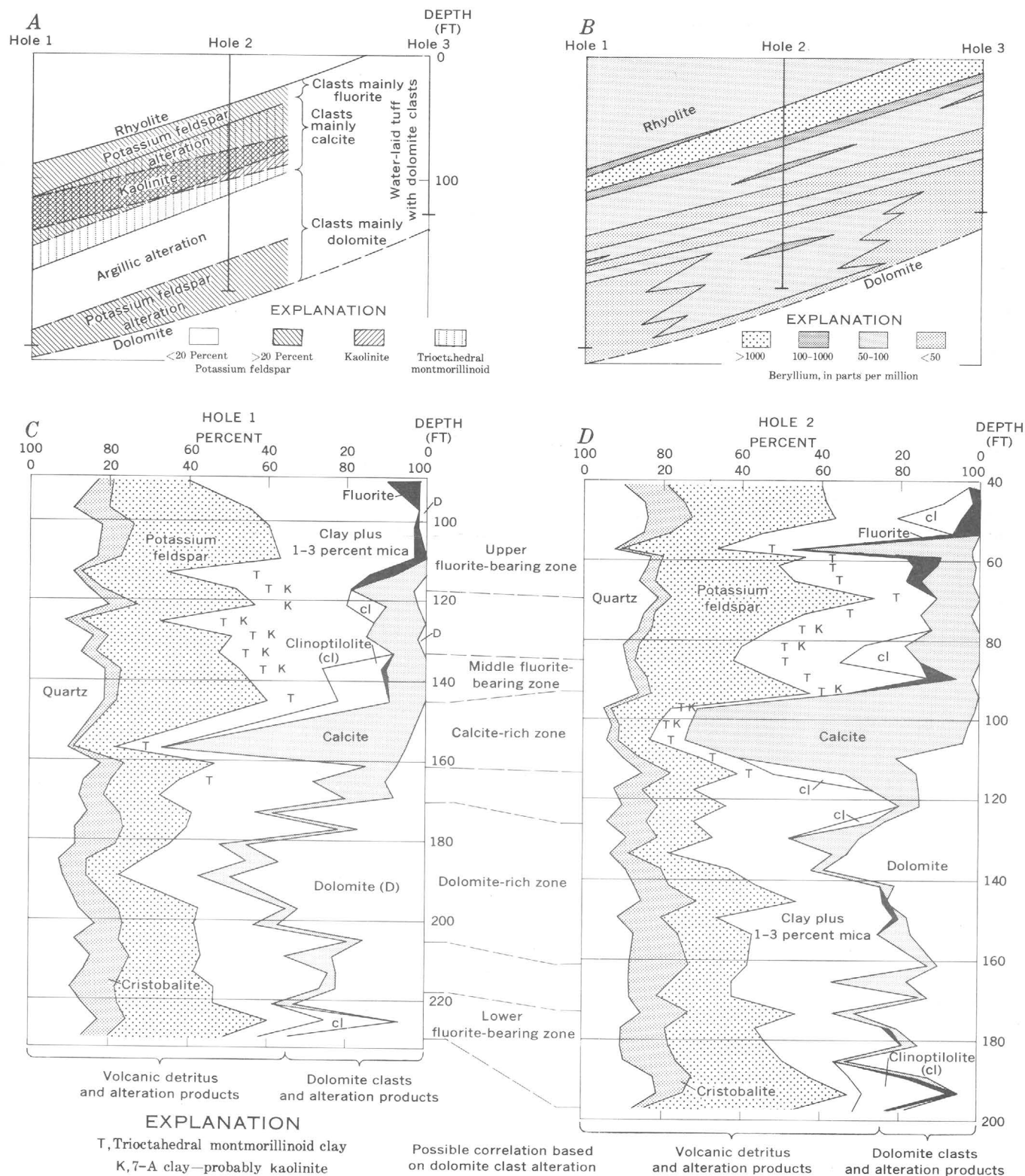

FIGURE 6. — Alteration patterns in the water-laid tuff at the Roadside beryllium deposit. A, Summary of the distribution of alteration minerals. B, Distribution of beryllium from Griffitts and Rader (1963, fig. 1). C, Profile of mineralogy cut by drill hole 1. D, Profile of mineralogy cut by drill hole 2. Mineralogy determined by X-ray diffraction.

part of a zone of feldspathic alteration and is directly above most of the lithium-bearing trioctahedral montmorillonoid clay and calcite zone. The lower zone of feldspathic alteration, which does not show extensive alteration of dolomite clasts, contains no large concentration of beryllium.

Contrary to the relationships shown by other minerals, a 7-A clay mineral thought to be kaolinite does not show a concordant distribution. The kaolinite zone clearly transects the calcite-dolomite boundary and is more nearly parallel to the topographic surface than to the zones of other minerals. It evidently reflects a later stage in alteration, possibly related to supergene processes.

ALTERATION NODULES IN TUFF

CALCITE-SILICA-FLUORITE NODULES

Subspherical nodules as much as 1 foot in diameter are commonplace and are characteristic of the altered tuff at the Roadside and other beryllium deposits at Spor Mountain. Figure 7 illustrates a sequence of typical nodules representing progressive stages of alteration, with details of mineralogy and chemistry. Some nodules exhibit complex alteration patterns, but many consist of concentric zones of calcite, microcrystalline quartz (chalcedony), opal, and fluorite, passing from core to rim. All the minerals are fine grained, and the fluorite ranges from purple to colorless. Numerous small nodules that consist only of alternating opal- and fluorite-rich zones are inferred to represent more advanced alteration. Relict bedding, invertebrate fossil fragments, and carbonate rock textures are seen in thin sections of the calcite cores of some nodules, confirming the earlier statement that the nodules are mainly the result of replacement of the original dolomite clasts. Twelve nodules from the Roadside beryllium deposit were selected for detailed mineralogical and chemical study in order to assess alteration patterns independently. The nodules were sawed into slabs, and 89 small samples of 1-2 grams each were cut from the various layers in the nodules. Each sample was studied by X-ray diffraction and analyzed by semiquantitative spectrographic methods.

The mineralogy and chemical composition of the Roadside nodules are summarized in table 2. The 89 sample analyses were grouped according to major mineralogy; those having 10 percent or more calcite were compiled into one group, those having 10 percent or more quartz were compiled into another group, and so on. By necessity, this resulted in some samples being included in more than one group, but for the most part the groups adequately represent the four mineral zones of calcite, quartz, opal, and fluorite, passing from core to rim in the idealized nodule. Median values (50th percentiles) were then computed for each element in each group. The median mineral content for each group as tabulated in table 2 reveals that the calcite- quartz-rich samples are nearly pure, containing only 10-20 percent other minerals. The opal and fluorite zones are less effec-

FIGURE 7 (facing page). — Calcite-silica-fluorite nodules from the Roadside beryllium deposit, selected to show progressive stages of alteration. Mineral zones in nodules are labeled as follows: ca, calcite; qz, quartz; op, opal; fl, fluorite; op-fl, opal with lesser fluorite; fl-op, fluorite with lesser opal; op-qz-fl, opal, quartz, and fluorite, in decreasing order of abundance. A, Nodule with calcite core (200 ppm Be), dark quartz zone (300 ppm Be), and outer light opal zone (as much as 2,000 ppm Be, 200 ppm Li) with minor fluorite. B, Nodule with white calcite core (as much as 500 ppm Be, 700 ppm Li, and 2,000 ppm Zn), gray quartz zone (as much as 500 ppm Be, 50 ppm Li, and 700 ppm Zn), and outer white zone of opal with as much as 15 percent fluorite (7,000 ppm Be, 1,000 ppm Li, and 10,000 ppm Zn). Nodule is crosscut by sponge-spicule-bearing chert concretion with manganese oxide fracture fillings containing as much as 70 ppm Be and 70 ppm Ag. C, Nodule with large gray quartz core (1,000 ppm Be) and outer light zone of opal with as much as 15 percent fluorite at the margin (as much as 5,000 ppm Be and 150 ppm Li). Dark spots are manganese oxides. D, Nodule with dark core of opal, quartz, and fluorite (10,000 ppm Be), brown and light patchy zone of opal and fluorite (as much as 10,000 ppm Be, 1,000 ppm U, and 1,000 ppm Mn), and outer light-purple rim of opal and fluorite (20,000 ppm Be, 150 ppm Li, and 1,500 ppm Mn locally). E, Left nodule with light- purple core of fluorite and opal (15,000 ppm Be, 200 ppm Li, and 500 ppm U), a dark-purple zone of nearly pure fluorite (10,000 ppm Be and 1,500 ppm U), and an opal-and-fluorite rim (10,000 ppm Be, 200 ppm Li, and 500 ppm U). Right nodule with dark-purple core of nearly pure fluorite (300 ppm Be and 700 ppm U), light-purple zone of fluorite and opal (10,000−20,000 ppm Be and 1,000−1,500 ppm U), and outer dark-purple zone of nearly pure fluorite (10,000 ppm Be and 2,000 ppm U). F, Fluorite and opal nodule with outer lavender zone containing as much as 20,000 ppm Be and 200 ppm Li. Light spots in lower half are spherulitic silica; dark patches in upper half are manganese oxides (all contain more than 1,000 ppm Be).

tively separated because of the finely intergrown nature of the two minerals as can be seen in thin sections.

The fluorite- and opal-rich zones, as shown by the chemical data in table 2, contain at least twice as much of the minor elements Na, Ti, As, B, Be, La, Li, Pb, Sr, U, Y, Yb, and Zn as do the calcite-rich zones. The calcite-rich zones, on the other hand, contain more Ba, Cd, Cu, and Mn than do the fluorite- and opal-rich zones. The quartz zones are generally the most impoverished in trace-element content, with the exception of Mo and Cu. Perhaps the most noteworthy concentrations of elements are those of Be, Li, U, and, locally, Zn, in the opal and fluorite zones and of Mn in the calcite zones.

Six samples containing more than 1 percent Be were selected for identification of beryllium minerals. All the samples were mixtures of opal and fluorite, but in each sample the fluorite content ranged from 50 to nearly 100 percent. The samples were boiled in concentrated, acidified $AlCl_3$ for about 15 minutes to remove the fluorite (Stevens and others, 1962). The residue was washed repeatedly, dried, and X-rayed. All the residues contained opal and bertrandite. Attempts to identify other beryllium minerals which might be present in lesser amounts than bertrandite were unsuccessful.

FLUORITE-CLAY-MANGANESE OXIDE NODULES

Fluorite-clay-manganese oxide nodules are locally abundant in the zone of feldspathic alteration. Twelve specimens
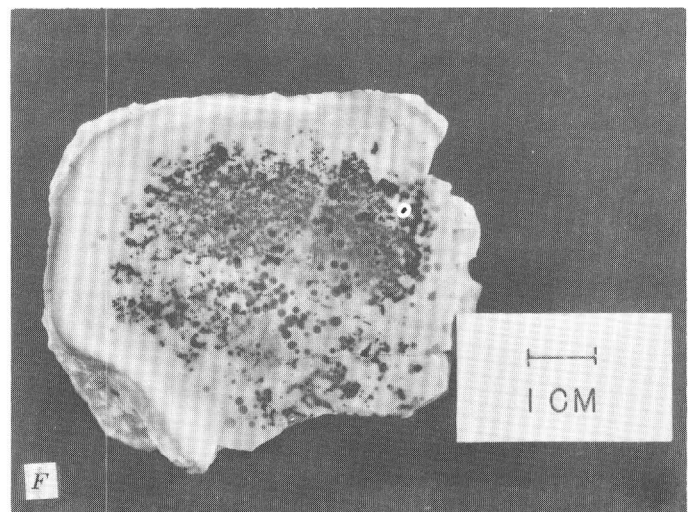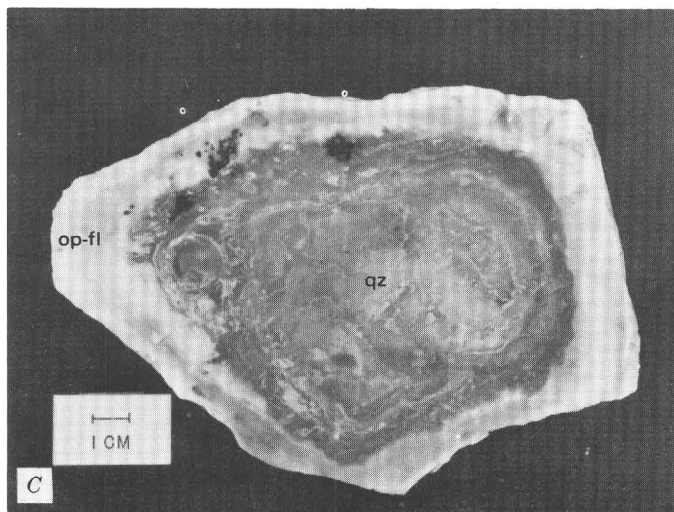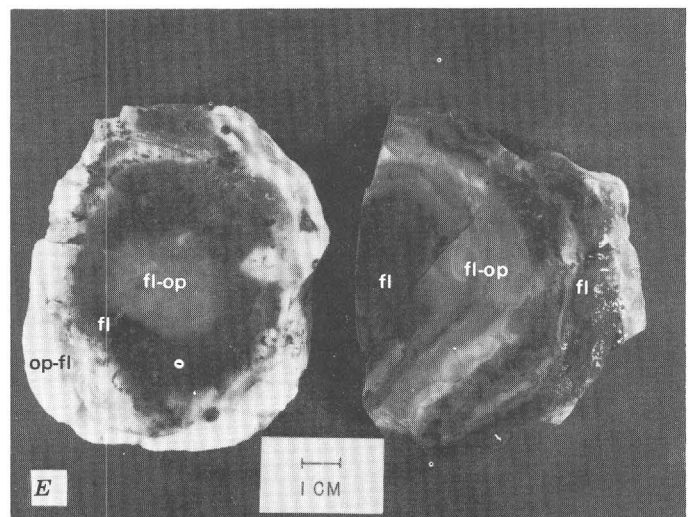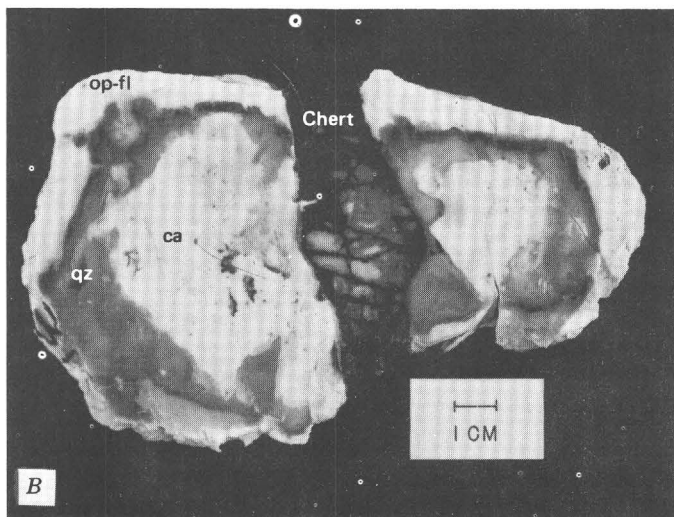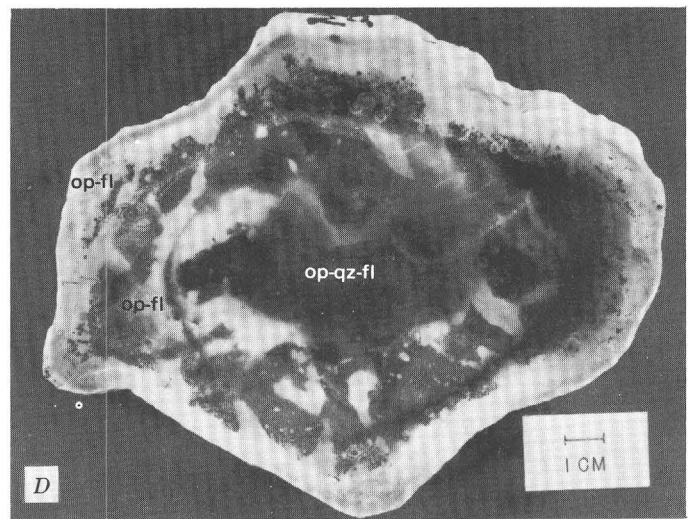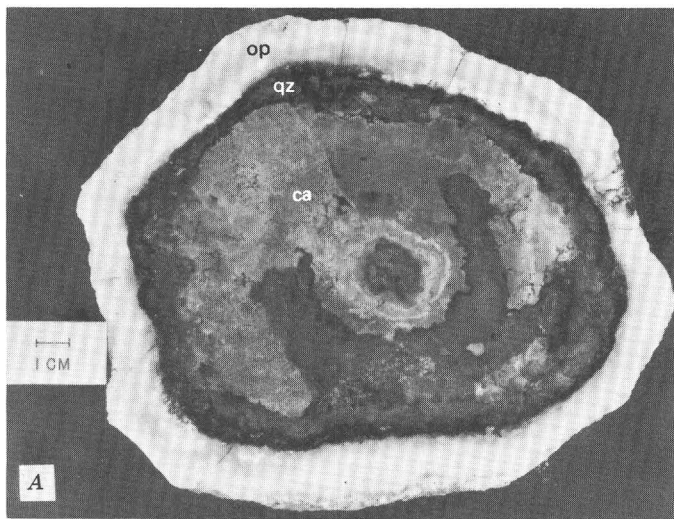
TABLE 2. — *Distribution of elements with respect to gross mineralogy in 12 calcite-silica-fluorite nodules from the Roadside beryllium deposit*

[The four mineralogic groups correspond roughly to the four zones from core to rim of some nodules. All values are medians (50th percentiles) expressed as weight percent or parts per million; where the median fell below the limit of detection, the maximum value (in parentheses) is recorded also. Bulk density calculated from mineral composition assuming zero porosity. Mineral composition, determined by X-ray diffraction. Chemical composition determined by six-step semiquantitative spectrographic analysis by L. A. Bradley. Elements looked for but not found, and their detection limits, are: Au, 20 ppm; Hf, 100 ppm; In, 10 ppm; P, 0.2 percent; Pd, 1 ppm; Pt, 30 ppm; Re, 30 ppm; Sb, 150 ppm; Sc, 5 ppm; Ta, 200 ppm; Te, 2,000 ppm; and Th, 200 ppm]

Zone (from core to rim of idealized nodule)	1	2	3	4
Major mineral (≥10 percent present)	Calcite	Quartz	Opal	Fluorite
Number of samples	22	29	47	33
Bulk density (g/cc; calculated)	2.70	2.60	2.37	2.64

Mineral composition (in percent)				
Calcite	90	10	<1	0
Quartz	10	80	10	<1
Opal	<1	10	70	50
Fluorite	<1	<1	20	50

Chemical composition (weight percent)							
Si	6		>10		>10		10
Al	.29		.34		.39		.41
Fe	.10		.06		.07		.06
Mg	.30		.10		.27		.25
Ca	>10		1.62		>10		>10
Na	.06		.05		.12		.13
K	<.7		<.7		<.7	(0.7)	<.7	(0.7)
Ti	.002		.002		.004		.004

Chemical composition (parts per million)							
Ag	<0.5	(1.5)	<0.5	(70)	<0.5	(3)	<0.5	(7)
As	<1,000		<1,000		<1,000	(3,000)	<1,000	(3,000)
B	<20		37		44		54
Ba	38		10		11		12
Be	162		359		5,843		10,436
Bi	<10		<10		<10	(20)	<10	(20)
Cd	28		<20	(70)	<20	(20)	<20
Ce	<150		<150		<150	(300)	<150	(300)
Co	<3		<3		<3	(10)	<3	(10)
Cr	2		1		2		1
Cu	7		9		4		3
Ga	<5		<5		<5	(10)	<5	(10)
Ge	<10		<10	(15)	<10	(15)	<10
La	<30		<30		<30	(300)	57
Li	<50	(700)	<50	(150)	90		87
Mn	1,000		1,100		88		60
Mo	6		12		3		3	(10)
Nb	<10	(20)	9		12		12
Ni	<5	(7)	<5	(10)	<5	(7)	<5	(5)
Pb	14		11		17		36
Sn	<10		<10	(15)	<10	(30)	<10	(30)
Sr	68		17		67		117
Tl	<50	(300)	<50	(300)	<50	(300)	<50	(150)
U	<500		<500		<500	(2,000)	536
V	<7	(10)	<7		<7	(30)	<7	(30)
W	<100		<100	(150)	<100	(150)	<100
Y	13		11		37		75
Yb	2		2		4		6
Zn	<200		<200	(700)	<200	(10,000)	<200	(10,000)
Zr	<10	(15)	<10	(15)	9		9

of nodule-bearing tuff from the Roadside and Rainbow deposits were selected for X-ray diffraction and spectrographic analysis. From the 12 specimens, 74 samples of 1-2 grams each were handpicked to represent various mineral zones observed in the nodules. Fluorite, clay, and manganese oxides were found to compose the major mineral components of the zones, but the zones themselves do not indicate a single alteration sequence. Thus some nodules have fluorite cores and clay rinds, others have fluorite cores enclosed by a clay zone and a manganese oxide rind, and

still others have clay-fluorite cores and fluorite-potassium feldspar-clay rinds (fig. 8). The manganese oxides in every sample examined appear to have been deposited as rinds or fracture fillings within the nodules; hence they were the last formed. Manganese oxide minerals identified by X-ray diffraction and spectrographic analysis are pyrolusite, cryptomelane, chalcophanite, and todorokite(?).

The most significant geochemical feature of the fluorite-clay-manganese oxide nodules is the high concentration of some elements, notably Be, Li, Mg, Mn, and Zn (fig. 8). Many of the cores contain dioctahedral montmorillonoid clay, but some also contain trioctahedral montmorillonoid clay with abundant Mg, Li, and Zn (fig. 8A). Beryllium, although it is abundant in some trioctahedral montmorillonoid-clay-bearing nodules, is not associated with all the clays, as shown by analysis of the large nodule in figure 8A. Generally the distribution of beryllium is not governed by zoning in the fluorite-clay-manganese oxide nodules; if it is abundant in the tuff matrix, it is abundant in most of the zones. Many of the manganese oxide rinds are chalcophanite and contain abundant zinc. Uranium (≥500 ppm) was found in only two specimens (fig. 8D), where it is mainly concentrated in the clay-fluorite rinds of nodules.

DISCUSSION AND CONCLUSIONS

ALTERATION PROCESSES

Evaluation of chemical changes involved in the alteration of rock at Spor Mountain provides keys to understanding the chemical reactions that took place. Although gains and losses of components can be surmised from the data in tables 1 and 2, it is more realistic to recalculate weight-percent data into gram-atoms or gram equivalents per unit volume (Hemley and Jones, 1964). Gram equivalents for oxide components were calculated by the formula:

$$\frac{g \text{ equiv}}{1,000 \text{ cc rock}} = \frac{\frac{\text{wt percent}}{100} \times \text{bulk density in g/cc} \times 1,000 \text{ cc}}{g \text{ molecular wt}} \times \frac{g\text{-atoms}}{\text{moles of oxide}} \times \text{valence};$$

and for elements, by the formula

$$\frac{g \text{ equiv}}{1,000 \text{ cc rock}} = \frac{\frac{\text{wt percent}}{100} \times \text{bulk density in g/cc} \times 1,000 \text{ cc}}{g \text{ atomic wt}} \times \text{valence}.$$

This procedure is advantageous in that it reduces gain-and-loss data to atomic proportions useful for inferring chemical reactions of alteration. Conversion of weight-percent analyses into gram equivalents per unit volume presumes that alteration proceeded without appreciable change in rock volume; this assumption is probably justified for the water-laid tuffs and carbonate clasts at Spor Mountain because of abundant undeformed relict structures in altered rock. Bulk- and powder-density data show that alteration of vitric tuff to argillic and feldspathic tuff is accompanied by appreciable decrease in porosity (table 1); that is, while volume remained constant, the mass of 1,000 cc of rock increased by filling of pore space. Thin-section study showed that porosity of the carbonate clasts remained low

throughout alteration. Gains and losses during clast alteration were approximated using bulk density computed from mineral composition and assuming zero porosity. Gains and losses of major components in the clasts were calculated from mineralogy because the maximum limit of detection

is complicated by differing original compositions; the mineralized tuff originally contained dolomite clasts not present in the unmineralized vitric tuff studied (table 1). The Mg^{+2}, Ca^{+2}, and CO_3^{-2} in dolomite clasts should be ignored, and these also cause an apparent dilution of other
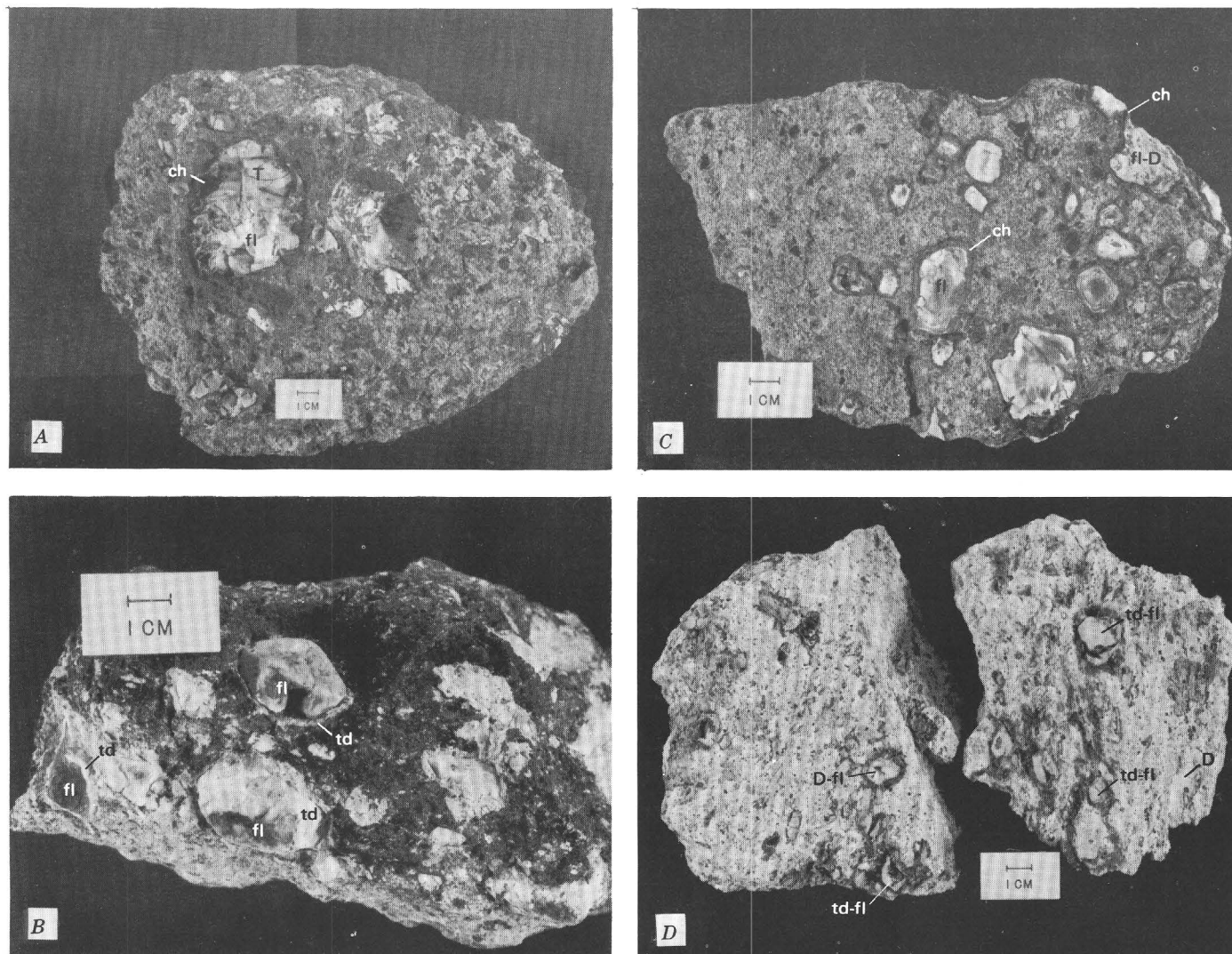

FIGURE 8. — Fluorite-clay-manganese oxide nodules from the Roadside and Rainbow beryllium deposits. All samples shown are from the zone of feldspathic alteration. Mineral zones in nodules are labeled as follows: fl, fluorite; T, trioctahedral montmorillonoid clay; D, dioctahedral montmorillonoid clay; td, both clays; ch, chalcophanite. A, Nodules with white fluorite cores, trioctahedral montmorillonoid clay zone, and manganese oxides (chalcophanite and todorokite(?)) rind. Manganese oxides also fill fractures in interior of nodules. Trioctahedral montmorillonoid clay contains 10 percent Mg, 3,000 ppm Li, 5,000 ppm Zn, and only 10−30 ppm Be. B, Nodules with purple fluorite core and thin rind of both dioctahedral and trioctahedral montmorillonoid clay. Clay

rinds contain as much as 3 percent Mg, 1,500 ppm Li, and 1,000 ppm Zn; beryllium can exceed 5,000 ppm in both cores and rinds. C, Nodules with fluorite and mixed fluorite-clay cores (dioctahedral montmorillonoid clay) and thin chalcophanite rinds. Cores have more than 5,000 ppm Be, 200−700 ppm Li, and 2,000 ppm Zn. D, Clay-rich nodules with purple rinds. Cores contain dioctahedral montmorillonoid clay and lesser fluorite; some also contain trioctahedral montmorillonoid clay and abundant sericite. Purple rinds contain abundant fluorite, potassium feldspar, and clay and minor opal, quartz, and sericite. Rinds contain as much as 2,000 ppm U but only 50−150 ppm Be.

by spectrographic analysis was often exceeded. The resulting data on major chemical gains and losses during alteration are summarized in table 3.

Determination of gains and losses accompanying alteration of vitric tuff to mineralized tuff (argillic or feldspathic)

components. Small apparent losses may have been due to dilution, and any gain registered by other components should be considered a minimum value. Chemical aspects of more advanced alteration may be evaluated independently by comparing the argillic with the feldspathic tuffs because these tuffs probably shared a similar original composition.

TABLE 3. — *Major chemical gains and losses per 1,000 cc of rock as shown by alteration of water-laid tuff and carbonate clasts in tuffs, Spor Mountain and the Thomas Range, Utah*

[Carbonate clasts in tuff: calculations for Si, Ca^{+2}, CO_3^{-2}, and F^- and sum of anions based on mineralogy; for K^+, no gain or loss was calculable because element abundance was generally below the limit of detection; n.d., no data available; Cl^- was presumed to be minor when calculating sum of anions]

Alteration	Si	Al	Ti	Fe^{+3}	Mn^{+2}	Mg^{+2}	Ca^{+2}	Be^{+2}	Na^+	K^+	Li^+	Sum of alkalis + alkaline earths	Moles H_2O (maximum)	CO_3^{-2}	Cl^-	F^-	Sum of anions
	Gram-atoms			Gram equivalents										Gram equivalents			
Water-laid tuff																	
Vitric to argillic _ _ _ _ _ _ _	2.93	1.13	−0.01	0.30	0	'1.28	'0.67	0.04	0.12	−0.26	0.05	'1.90	3.85	0.05	0.15	1.03	1.23
Argillic to feldspathic _ _ _ _ _	−.43	−.09	0	0	.02	−.54	.25	−.03	−.04	.91	.02	.57	−2.01	−.33	−.08	.55	.14
Carbonate clasts in tuff																	
Calcite to quartz _ _ _ _ _ _ _	34.01	0.08	0	−0.08	−0.09	−0.46	−43.38	0.10	−0.03	_ _ _ _	0	−43.77	n.d.	·−43.36	n.d.	0	−43.36
Quartz to opal _ _ _ _ _ _ _ _	−9.72	.03	0	.01	0	.32	6.74	2.87	.13	_ _ _ _	.01	10.07	n.d.	−4.73	n.d.	11.44	6.71
Opal to fluorite _ _ _ _ _ _ _	−9.02	.11	0	−.01	0	.01	21.20	3.05	.05	_ _ _ _	0	24.31	n.d.	−.47	n.d.	21.68	21.21
Calcite to fluorite _ _ _ _ _ _	15.27	.22	0	−.08	−.09	−.13	−15.44	6.02	.16	_ _ _ _	.01	−9.38	n.d.	−48.56	n.d.	33.12	−15.44

'Value due mainly to different original composition.

The first stage of the mineralizing event is believed to have been argillization of vitric tuff to form tuff containing dioctahedral montmorillonoid clay; this entailed mainly addition of Si, Al, Fe^{+3}, H_2O, and F^- and loss of K^+. (The valence of Fe is assumed to be +3; Fe^{+2} may have participated.) Lesser amounts of Be^{+2}, Li^+, and Cl^- also were added. Although meaningful gain-loss calculations are not possible for Mg^{+2}, Ca^{+2}, and CO_3^{-2}, argillization took place in an environment rich in these ions. Hydrolysis of silicates (or, in this case, rhyolitic glass) to form montmorillonoid clay is favored by an environment with an adequate supply of Mg^{+2}, Ca^{+2}, Fe^{+2}, and Na^+ relative to H^+, high Si relative to Al, and low K^+ relative to other alkali and alkaline earth cations (Keller, 1970, p. 800). Inspection of the gain-loss data in table 3 for transformation of vitric to argillic tuff shows that nearly all of these conditions were present. A possible reaction is:

rhyolite glass $+ \frac{1}{2} Mg^{+2} + 3 H_2O$
$\longrightarrow$ 2 dioctahedral montmorillonoid clay + 9 opal + K^+. (1)
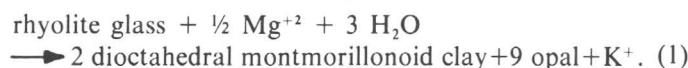
The equation can be balanced only approximately, but it takes into account the actual composition of the rhyolite glass as indicated by the vitric tuff. Hydrolysis of glass and leaching of K^+ were probably important processes. Only a slight increase in cristobalite and opal was noted in the argillic tuff; some of the silica probably remained in solution and was precipitated later in the feldspathic tuff, or it replaced nearby carbonate clasts. The proposed reaction also requires addition of Mg^{+2}, perhaps derived from alteration of dolomite clasts. Calcium ion and Na^+ derived from the glass may have been held as exchangeable cations in the clay lattice.
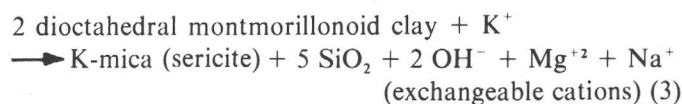
The presence of calcite and lithium-bearing trioctahedral montmorillonoid clay correlates with the absence of dolomite in the drill samples at the Roadside pit (fig. 6); this observation indicates that another argillization reaction may al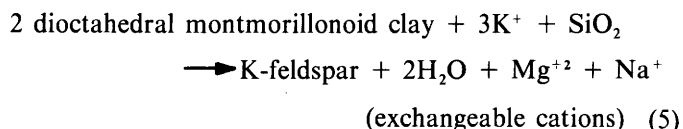so have occurred. The distribution of calcite and trioctahedral montmorillonoid clay overlaps into the feldspathic zone, indicating that the reaction proceeded also during feldspathization. The reactions must have involved the leaching of dolomite to form calcite:

dolomite $+ H_2O \longrightarrow$ calcite $+ Mg^{+2}$
$+ HCO_3^- + OH^-$. (2)
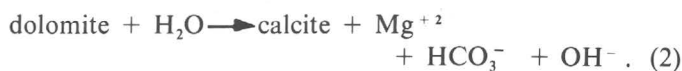
Reaction 2 released Mg^{+2} and increased the alkalinity of the solutions. Lithium, supplied by solution, and Mg^{+2} may then have displaced Al^{+3} in dioctahedral montmorillonoid clay to produce a lithium-bearing trioctahedral montmorillonoid clay similar to hectorite. Disposal of Al^{+3} from the latter reaction is an unsolved problem; gibbsite and other aluminous minerals were not found, and it is doubtful if appreciable quantities of these minerals could have gone undetected by X-ray methods. A similar reaction involving addition of Mg^{+2} to dioctahedral montmorillonite to produce saponite and other products was studied in the laboratory by Ames and Sand (1958). They showed that, with optimum substitution in the clay lattice, dioctahedral montmorillonite is converted to saponite at 480°C, and that saponite and hectorite are stable to as much as 750°C. The temperature-stability limit of both clays is much lower when optimum substitution is not achieved. Probably, therefore, conversion of dioctahedral to trioctahedral montmorillonoid clay was driven by an increase in temperature.

Advanced alteration of argillic to feldspathic tuff was accompanied mainly by addition of K^+, Ca^{+2}, and F^- and by loss of Si, Mg^{+2}, CO_3^{-2}, and appreciable H_2O. The following approximate equations suggest the principal reactions during feldspathization:

2 dioctahedral montmorillonoid clay $+ K^+$
$\longrightarrow$ K-mica (sericite) $+ 5 SiO_2 + 2 OH^- + Mg^{+2} + Na^+$
(exchangeable cations) (3)

K-mica $+ 6SiO_2 + 2K^+ + 2OH^-$
$\longrightarrow$ 3 K-feldspar $+ 2H_2O$ (4)

2 dioctahedral montmorillonoid clay + $3K^+$ + SiO_2

$$\longrightarrow \text{K-feldspar} + 2H_2O + Mg^{+2} + Na^+$$

(exchangeable cations)   (5)

Evidence for reaction 3 is clearly visible in figures 4D and 5F, where sericite is seen to have formed on clay-rich clasts. This reaction probably began during argillic alteration. Reaction 5 is merely the sum of 3 and 4, and reveals that the net effect to be expected from feldspathization of argillic tuff is the considerable addition of K^+ and some Si accompanied by loss of H_2O, Mg $^{+2}$, and exchangeable cations (Na^+, Mg^{+2}, Ca ^{2}) as these become available for removal in solutions. Except for the relatively small loss recorded for Si, the gain-loss data for argillic to feldspathic tuff correspond remarkably well to the effects of reaction 5. Although some of the K involved in feldspathization may have been derived from argillic alteration of the original glass, the overall gain in K^+ suggests that some was added from an external source. Study of reaction 4 by Hemley (1959) showed that, at 300°C and above, formation of kaolinite, potassium mica, and potassium feldspar is favored by progressively higher K^+/H^+ ratios as well as by higher temperatures. Potassium feldspar is stable at lower (25°C) temperatures but only at extremely high K^+/H^+ ratios of approximately 10^9-10^{10} (Garrels and Howard, 1959). Although reactions 3, 4, and 5 were probably favored by increased temperatures at Spor Mountain, rising pH, probably caused by release and hydrolysis of CO_3^{-2} as the solutions altered carbonate clasts, was probably the mechanism which triggered feldspathization.

Study of the carbonate clasts is particularly informative regarding the solubility of calcite, silica, and fluorite in the mineralizing solutions. The interpretation of alteration of carbonate clasts (table 3) covers only the calcite-silica-fluorite stages because those clasts studied did not retain any dolomite. No information is now available on the minor-element composition of the original dolomite clasts. The gain-loss data show the almost total progressive transformation from high $CaCO_3$ to SiO_2 to CaF_2 as computed from mineralogy. Alteration of [the calcite cores of] the clasts to fluorite contributed to the solutions major quantities of Ca $^{+2}$, Mg $^{+2}$, and CO_3 $^{-2}$ and minor, but significant, quantities of Fe $^{+3}$ and Mn $^{+2}$ while extracting from solution major amounts of Si, Be $^{+2}$, and F^- as well as minor amounts of Al, Na^+, Li^+, and, of course, the many other trace elements listed in table 2. Judged from the associated clay mineralogy, solution of calcite was probably accomplished by neutral or slightly alkaline solutions which became more alkaline as carbonate ions released into solution were hydrolyzed to produce bicarbonate and OH^- Although calcite is more readily dissolved under acid conditions, Ames (1961) has shown that fluorite can replace limestone under alkaline conditions. The alteration sequence in the nodules indicates that SiO_2 saturation with

respect to quartz occurred before general saturation with respect to CaF_2, and that as alteration progressed, the environment became supersaturated with respect to quartz (precipitation of opal). Temperature and pressure, as shown by experimental studies, are major influences on silica solubility under the pH conditions usually present in geological environments (Holland, 1967, p. 388–393). Inasmuch as silica replacement was local and sporadic, forming nodules, we can reasonably appeal to decreasing temperature as the mechanism for nodule silicification. Below 100°C in pure water, and at higher temperatures in electrolyte solutions, fluorite can also be precipitated by decreasing temperature (Holland, 1967, p. 395). The fine-grained intergrowth of fluorite with opal in the nodules indicates that both were precipitated together under the same conditions, although the solubility of fluorite was additionally complicated by complexing, as will be discussed later. Decreasing temperature of the mineralizing solutions may also explain the pronounced upward decrease of cristobalite observed in the drill-hole samples of altered tuff.

All the preceding reactions are thought to be hypogene processes. The role of supergene processes, controlled by past or present water tables, is difficult to assess. The kaolinite zone observed in the Roadside drill samples does not harmonize with the rest of the mineralogy of the altered tuff, inasmuch as it indicates a more acid stage of alteration. The kaolinite zone is discordant to the bedding and appears to have been overprinted on the other alteration zones, all of which are concordant. It may be related to the position of some past or present water table.

CHEMICAL TRANSPORT AND PRECIPITATION MECHANISMS

The mechanism for transportation and precipitation of Be, Li, U, Mn, and certain other elements at Spor Mountain remains speculative, but the main possibilities can be explored. Staatz and Griffitts (1961, p. 949; Staatz, 1963, p. M34) suggested that Be, Mn, U, and certain other elements were transported in solution as soluble fluoride complex ions, and that their precipitation occurred when formation of fluorite caused a decrease in fluorine concentration sufficient to render the complexes unstable. This mechanism could account for the association of Be, U, and other elements with fluorite, as demonstrated in the study of the calcite-silica-fluorite nodules. We have shown, however, that the alteration process has released large quantities of carbonate and bicarbonate ions which probably increased the alkalinity of the mineralizing solutions (table 3). These ions are known to form stable complexes with beryllium (Govorov and Stunzhas, 1963), uranium (Miller, 1958; Naumov, 1959; Hostetler and Garrels, 1962), and manganese (Hem, 1963). These complexes may be destroyed by various means, including decrease of a carbonate species (that is, by precipitation of insoluble carbonates, escape of CO_2 through fractures, and acidification

with resulting production of CO_2), precipitation as an hydroxide if alkalinity increases, or, in the case of uranium, by reduction and precipitation of insoluble uranous compounds.

Beryllium fluoride (fluoroberyllate) complex ions are known; and according to Novoselova and Simanov (1955, and reported in Beus, 1966, p. 22), these complex ions disintegrate with increasing alkalinity, precipitating $Be(OH)_2$. Phenakite (Be_2SiO_4) has been produced in the laboratory from BeO and SiO_2 in the presence of beryllium fluoride complex ions (Sobolev and Novoselova, 1959). The halogen-bearing carbonatoberyllates studied by Govorov and Stunzhas (1963) are stable over a wide range of pH (7-11) and, when CO_2 is not allowed to escape, to temperatures exceeding 200°C. Beus (1966, p. 22), however, reported that the fluoride complex compounds are more stable than corresponding beryllium carbonate complex compounds. Recent work (Mesmer and Baes, 1969) has shown that BeF_4^{-2} and BeF_3^- ions are stable in acid and neutral solutions at fluoride concentrations of 10^{-2} mg/l (milligrams per liter) or less, and BeF^+ is stable in solution with fluoride concentrations of less than 10^{-4} mg/l. The various beryllium fluoride complexes are also stable in solution to at least 60°C. It seems likely, in view of the close beryllium-fluorine association at Spor Mountain, that beryllium was transported as a beryllium fluoride complex and precipitated by removal of fluorine from solution. Alternatively, if beryllium was transported as fluoride complex ions, precipitation may have occurred when the solutions became markedly alkaline. Experimental verification of this possibility is needed.

Uranyl dicarbonate and tricarbonate complex ions have a combined pH stability range of 4.5 to 11.5 and are stable at temperatures of at least 200°C (Miller, 1958, p. 536; Naumov, 1959, p. 17). Although the uranyl carbonate complexes are more stable at 25°C, the uranyl fluoride complex ion becomes the more stable complex ion at higher temperatures (Miller, 1958, p. 543). At 215°C the solubility of uranyl fluoride is several orders of magnitude larger than that of either uranyl carbonate complex. Hence, it seems likely, in view of the uranium-fluorine association noted at Spor Mountain, and in view of the presumed elevated temperatures, that uranium was also transported as the uranyl fluoride complex.

The solubility of manganese at 25°C in aqueous solutions is appreciably increased owing to formation of the soluble bicarbonate complex cation when the pH is favorable; at 2,000 ppm HCO_3^- the bicarbonate complex is stable over a pH range of 6.35 to 8.2 (Hem, 1963, p. A38-A43). Manganese also forms stable complexes with fluorine (Sillén, 1964, p. 261). As seen from the gain-loss data in table 3, manganese is removed from calcite during the early stage of silicification and is not returned during fluoritization. Instead, manganese is precipitated last as nodule coatings and fissure fillings. This evidence indicates that

manganese may not have been transported as a fluoride complex; inasmuch as it was leached from the nodules along with Ca^{+2} and CO_3^{-2}, the bicarbonate complex transport mechanism seems most likely. Rising alkalinity would cause precipitation of $MnCO_3$, which is then commonly oxidized to manganese oxides by later supergene processes.

Stable fluoride complexes with many other elements are known or suspected, including Si^{+4}, Al^{+3}, Ga^{+3}, B^{+3}, Fe^{+3}, Sn^{+2}, Zn^{+2}, and rare earth elements (Sillén, 1964, p. 256-267; Mesmer and Baes, 1969, p. 625-626). These elements are all demonstrated to have been mobile in the Spor Mountain alteration environment (tables 1, 2, and 3). In particular, the demonstrated mobility and addition of aluminum during alteration of the tuff and of the carbonate clasts is striking in view of the widely assumed immobility of this element. Beus (1966, p. 276) also noted that aluminum is mobilized commonly in the fluorine-rich acid environments of greisenization.

In summary, the foregoing discussion indicates that the mineralizing solutions at Spor Mountain were charged with abundant silicon, aluminum, alkali and alkaline earth metals, and fluorine. The mineralizing solutions were probably of low temperature (≤200°C) and neutral or slightly alkaline when they first entered the tuff; they became increasingly alkaline as they reacted with carbonate clasts in the tuff. Precipitation and fixation of these elements were variously caused by rising pH, declining fluorine concentration, and falling temperature.

ORIGIN OF THE SPOR MOUNTAIN BERYLLIUM DEPOSITS

The mineralizing solutions at Spor Mountain previously were thought to have been derived directly from the magma that formed the topaz rhyolite of the Thomas Range (Staatz, 1963, p. M33-M34). Indeed, the topaz rhyolite does contain anomalous trace quantities of Be, Mn, F, and U and undoubtedly is genetically related to the western Utah beryllium belt (Staatz, 1963; Shawe, 1966, tables 2 and 3). Three other lines of evidence, however, may pertain to the problem of the origin of the beryllium deposits: beryl-bearing granites, beryllium zonation in carbonate rocks, and the geologic setting of various types of beryllium deposits in western Utah.

Many of the elements shown to be mobile at Spor Mountain were also mobilized in the beryl deposits related to albitized and greisenized granites in Transbaikalia, Siberia (Beus, 1966, p. 255-280). There, alkali and alkaline earth metals, alumina, and beryllium were extracted from granite country rock by acid, fluorine-rich hydrothermal solutions. Decreasing temperature and acidity caused deposition of quartz, topaz, mica, and beryl as greisens and as fissure fillings. If these or similar solutions were to escape into overlying country rocks such as the tuffs at Spor Mountain, argillic, sericitic, and feldspathic alteration would be expected to occur. Beryllium and other elements remaining in solution could be deposited in the altered zones, as they were

at Spor Mountain. If the solutions moved into carbonate rocks, fluorite-silica replacement would be expected — for example, the fluorite pipes and altered nodules in tuff at Spor Mountain.

A complete sequence of alteration zones around granite intrusives in carbonate rocks has been recognized in the tin-beryllium deposits of Alaska (Sainsbury, 1969, p. 84-85). The sequence consists of six major zones grading outward from granite: greisen and skarn (two zones), transitional tin-beryllium-fluorite, beryllium-fluorite, fluorite-low-temperature sulfides, and fluorite-chalcedonic silica. Fluorite ranges from colorless in the inner zone to purple in the outer zone. According to the zonal gangue mineralogy and associated fluorite color proposed by Sainsbury, the Spor Mountain deposits belong to the outer, fluorite-chalcedonic silica zone. This conclusion is also in agreement with the incomplete alteration of vitric and zeolitic tuff at Spor Mountain to clays, sericite, and potassium feldspar. If the Spor Mountain deposit is correctly placed in Sainsbury's zonal classification, the distribution of bertrandite and manganese minerals needs to be extended into the outer zone. Bertrandite has also been reported as the only beryllium mineral in two other beryllium deposits — Aguachile Mountain, Mexico, and Apache Warm Springs, N. Mex. — which probably formed in low-temperature hydrothermal environments (Levinson, 1962; Hillard, 1969).

The source of the mineralizing solutions may be inferred from the surrounding intrusive and extrusive rocks in western Utah. The great volume of topaz rhyolite in the Thomas Range is evidence for a beryllium-, uranium-, and fluorine-rich magmatic source beneath the Spor Mountain beryllium and fluorite deposits, as discussed by Staatz (1963, p. M33-M34). The beryl-bearing granite of the Sheeprock Mountains lies only 40 miles to the northeast and may be a nearby analog to the source of the Spor Mountain solutions. The granite of the Sheeprock Mountains contains beryl, and related greisens also contain fluorite and topaz (Cohenour, 1959, p. 117-120; 1963b); the occurrence may be similar to the beryllium-bearing greisens described by Beus (1966). The Sheeprock granite is structurally high and is in contact with Precambrian and Paleozoic strata; consequently, it may provide a view of moderate to deep-level beryllium deposits in the western Utah belt. The Spor Mountain beryllium deposits, however, are within a structural low filled with volcanic rock; they represent the near-surface environment of beryllium deposits in western Utah.

The foregoing discussions of beryl-bearing granites in Siberia, beryllium zonation around granites in Alaska, and the possible variation in depth of different beryllium deposits in western Utah imply that the deposits at Spor Mountain may have been formed in a near-surface environment by solutions derived from intrusives beneath the Thomas Range. Leaching of the intrusives by ascending

fluorine-bearing solutions could bring silica, alumina, alkalis, beryllium, and other elements into the near-surface environment of porous tuffs and carbonate rocks. Here, rising pH, declining fluorine concentration, and falling temperature probably caused argillic and feldspathic alteration in the tuff and fluorite-silica replacement of carbonate rock accompanied by emplacement of beryllium deposits.

REFERENCES CITED

Ames, L. L., Jr., 1961, The metasomatic replacement of limestones by alkaline, fluoride-bearing solutions: Econ. Geology, v. 56, no. 4, p. 730-739.

Ames, L. L., Jr., and Sand, L. B., 1958, Factors effecting maximum hydrothermal stability in montmorillonites: Am. Mineralogist, v. 43, no. 7-8, p. 641-648.

Ames, L. L., Jr., Sand, L. B., and Goldich, S. S., 1958, A contribution on the Hector, California, bentonite deposit: Econ. Geology, v. 53, no. 1, p. 22-37.

Beus, A. A., 1966, Geochemistry of beryllium and genetic types of beryllium deposits: San Francisco, Freeman, 401 p.

Cohenour, R. E., 1959, Sheeprock Mountains, Tooele and Juab Counties: Utah Geol. and Mineralog. Survey Bull. 63, 201 p.

———1963a, The beryllium belt of western Utah, in Beryllium and uranium mineralization in western Juab County, Utah: Utah Geol. Soc. Guidebook to the Geology of Utah, no. 17, p. 4-7.

——— 1963b, Beryllium and associated mineralization in the Sheeprock Mountains, in Beryllium and uranium mineralization in western Juab County, Utah: Utah Geol. Soc. Guidebook to the Geology of Utah, no. 17, p. 8-13.

Crittenden, M. D., Jr., Straczek, J. A., and Roberts, R. J., 1961, Manganese deposits in the Drum Mountains, Juab and Millard Counties, Utah: U.S. Geol. Survey Bull. 1082-H, p. 493-544.

Eitel, Wilhelm, 1957, Structural anomalies in tridymite and cristobalite: Am. Ceramic Soc. Bull., v. 36, no. 4, p. 142-148.

Fowkes, E. J., 1964, Pegmatites of Granite Peak Mountain, Tooele County, Utah: Brigham Young Univ. Geology Studies, v. 11, p. 97-127.

Franks, P. C., and Swineford, Ada, 1959, Character and genesis of massive opal in Kimball Member, Ogallala Formation, Scott County, Kansas: Jour. Sed. Petrology, v. 29, no. 2, p. 186-196.

Garrels, R. M., and Howard, Peter, 1959, Reactions of feldspar and mica with water at low temperature and pressure, in Swineford, Ada, ed., Clays and clay minerals: Natl. Conf. Clays and Clay Minerals, 6th, Berkeley, Calif., Proc., v. 2, p. 68-88.

Govorov, I. N., and Stunzhas, A. A., 1963, Mode of transport of beryllium in alkali metasomatism: Geochemistry, v. 7, no. 4, p. 402-409.

Griffitts, W. R., 1964, Beryllium, in Mineral and water resources of Utah: Utah. Geol. and Mineralog. Survey Bull. 73, p. 71-75.

——— 1965, Recently discovered beryllium deposits near Gold Hill, Utah: Econ. Geology, v. 60, no. 6, p. 1298-1305.

Griffitts, W. R., and Rader, L. F., Jr., 1963, Beryllium and fluorine in mineralized tuff, Spor Mountain, Juab County, Utah, in Geological Survey research 1963: U.S. Geol. Survey Prof. Paper 475-B, p. B16-B17.

Hem, J. D., 1963, Chemical equilibria and rates of manganese oxidation: U.S. Geol. Survey Water-Supply Paper 1667-A, 64 p.

Hemley, J. J., 1959, Some mineralogical equilibria in the system K_2O-Al_2O_3-SiO_2-H_2O: Am. Jour. Sci., v. 257, no. 4, p. 241-270.

Hemley, J. J., and Jones, W. R., 1964, Chemical aspects of hydrothermal alteration with emphasis on hydrogen metasomatism: Econ. Geology, v. 59, no. 4, p. 538-567.

Hillard, P. D., 1969, Geology and beryllium mineralization near Apache Warm Springs, Socorro County, New Mexico: New Mexico Bur. Mines and Mineral Resources Circ. 103, 16 p.

Holland, H. D., 1967, Gangue minerals in hydrothermal deposits, *in* Barnes, H. L, ed., Geochemistry of hydrothermal ore deposits: New York, Holt, Rinehart and Winston, p. 382-436.

Hostetler, P. B., and Garrels, R. M., 1962, Transportation and precipitation of uranium and vanadium at low temperatures, with special reference to sandstone-type uranium deposits: Econ. Geology, v. 57, no. 2, p. 137-167.

Keller, W. D., 1970, Environmental aspects of clay minerals, *in* Symposium on environmental aspects of clay minerals: Jour. Sed. Petrology, v. 40, no. 3, p. 788-813.

Levinson, A. A., 1962, Beryllium-fluorine mineralization at Aguachile Mountain, Coahuila, Mexico: Am. Mineralogist, v. 47, nos. 1-2, p. 67-74.

Lindsey, D. A., and others, 1973, Mineralogical and chemical data for alteration studies, Spor Mountain beryllium deposits, Juab County, Utah: U.S. Geol. Survey Rept., p. 31, available only from U.S. Dept. Commerce Natl. Tech. Inf. Service, Springfield, Va. 22151, as Rept. PB−220−552, 24 p.

Mesmer, R. E., and Baes, C. F., Jr., 1969, Fluoride complexes of beryllium (II) in aqueous media: Inorganic Chemistry, v. 8, no. 3, p. 618-626.

Miller, L. J., 1958, The chemical environment of pitchblende: Econ. Geology, v. 53, no. 5, p. 521-545.

Montoya, J. W., Bauer, G. S., and Wilson, S. R., 1964, Mineralogical investigation of beryllium-bearing tuff, Honeycomb Hills, Juab County, Utah: U.S. Bur. Mines Rept. Inv. 6408, 11 p.

Montoya, J. W., Havens, R., and Bridges, D. W., 1962, Beryllium-bearing tuff from Spor Mountain, Utah — its chemical, mineralogical, and physical properties: U.S. Bur. Mines Rept. Inv. 6084, 15 p.

Mumpton, F. A., 1960, Clinoptilolite redefined: Am. Mineralogist, v. 45, nos. 3-4, p. 351-369.

Naumov, G. B., 1959, Transportation of uranium in hydrothermal solution as a carbonate: Geochemistry, v. 3, no. 1, p. 5-20.

Novoselova, A. V., and Simanov, Yu. T., 1955, Structure and transformation of fluoridic beryllium compounds: Uchenye zapiski of Moscow State Univ., issue 174 [in Russian].

Park, G. M., 1968, Some geochemical and geochronologic studies of the beryllium deposits in western Utah: Utah Univ. unpub. M.S. thesis, Salt Lake City, Utah, 105 p.

Ross, C. S., and Hendricks, S. B., 1945, Minerals of the montmorillonite group, their origin and relation to soils and clays: U.S. Geol. Survey Prof. Paper 205-B, p. 23-79 [1946].

Ross, C. S., and Smith, R. L., 1961, Ash-flow tuffs — their origin, geologic relations and identification: U.S. Geol. Survey Prof. Paper 366, 81 p.

Sainsbury, C. L., 1969, Geology and ore deposits of the central York Mountains, western Seward Peninsula, Alaska: U.S. Geol. Survey Bull. 1287, 101 p. [1970].

Shawe, D. R., 1966, Arizona-New Mexico and Nevada-Utah beryllium belts, *in* Geological Survey research 1966: U.S. Geol. Survey Prof. Paper 550-C, p. C206-C213.

_____ 1968, Geology of the Spor Mountain beryllium district, Utah, *in* v. 2 *of* Ore deposits of the United States, 1933-1967 (Graton-Sales Vol.): Am. Inst. Mining, Metall., and Petroleum Engineers, p. 1148-1161.

_____ 1972, Reconnaissance geology and mineral potential of Thomas, Keg, and Desert calderas, central Juab County, Utah, *in* Geological Survey research 1972: U.S. Geol. Survey Prof. Paper 800-B, p. B67-B77.

Shawe, D. R., Mountjoy, Wayne, and Duke, Walter, 1964, Lithium associated with beryllium in rhyolitic tuff at Spor Mountain, western Juab County, Utah, *in* Geological Survey research 1964; U.S. Geol. Survey Prof. Paper 501-C, p. C86-C87.

Sillén, L. G., 1964, Stability constants of metal-ion complexes, Sec. 1 — Inorganic ligands [2d ed.]: Chem. Soc. London Spec. Pub. 17, 754 p.

Sobolev, B. P., and Novoselova, A. V., 1959, The role of fluorine compounds in the transportation of beryllium and the formation of phenakite: Geochemistry, v. 3, no. 1, p. 21-32.

Staatz, M. H., 1963, Geology of the beryllium deposits in the Thomas Range, Juab County, Utah: U.S. Geol. Survey Bull. 1142-M, 36 p.

Staatz, M. H., and Carr, W. J., 1964, Geology and mineral deposits of the Thomas and Dugway Ranges, Juab and Tooele Counties, Utah: U.S. Geol. Survey Prof. Paper 415, 188 p.

Staatz, M. H., and Griffitts, W. R., 1961, Beryllium-bearing tuff in the Thomas Range, Juab County, Utah: Econ. Geology, v. 56, no. 5, p. 941-950.

Stevens, R. E., Sainsbury, C. L., and Bettiga, A. C., 1962, Dissolving fluorite with solutions of aluminum salts, *in* Geological Survey research 1962: U.S. Geol. Survey Prof. Paper 450-C, p. C98-C99.

Thurston, W. R., Staatz, M. H., Cox, D. C., and others, 1954, Fluorspar deposits of Utah: U.S. Geol. Survey Bull. 1005, 53 p.

Williams, N. C., 1963, Beryllium deposits, Spor Mountain, Utah, *in* Beryllium and uranium mineralization in western Juab County, Utah: Utah Geol. Soc. Guidebook to the Geology of Utah, no. 17, p. 36-59.

Wright, T. L., 1968, X-ray and optical study of alkali feldspar — [pt.] 2, An X-ray method for determining the composition and structural state from measurement of 2Θ values for three reflections: Am. Mineralogist, v. 53, nos. 1-2, p. 88-104.